Drivers of high rates of carbon burial in a riverine-influenced freshwater marsh in the Lake Erie watershed of southern Ontario, Canada

Amanda Lily Loder[1], Adam Gillespie[2], Omid Haeri Ardakani[3], and Sarah A Finkelstein[1]

[1]University of Toronto
[2]University of Guelph
[3]Natural Resources Canada

March 9, 2023

Abstract

Freshwater marshes are prevalent and important stores of carbon. They bury carbon in deeper soils, although reported rates of carbon accumulation are significantly higher over recent (decadal) versus longer (centennial and millennial) timescales. Intrinsic organic matter degradation, long-term climatic and ecological changes, and recent anthropogenic impacts on sediment fluxes and organic matter production may have a role in explaining this discrepancy, yet remain poorly understood for freshwater marshes. We collected a 4-m core from a riverine-influenced marsh in the watershed of Big Creek which drains into Lake Erie in southern Ontario, Canada, and conducted radiometric dating, elemental analyses, and programmed pyrolysis for organic matter characterization. Over the past 5,710 calibrated years, burial of organic (on average 26 ± 34 g C m-2 yr-1) and inorganic (22 ± 25 g C m-2 yr-1) carbon fractions has resulted in high rates of carbon accumulation. We found that elevated recent rates of organic carbon accumulation are driven by fractions that have low thermal stability and are predominantly from aquatic sources. This type of organic carbon is buried intermittently in deeper marsh sediments and corresponds to major hydro-fluvial events (e.g., Nipissing highstands), which coincide with regional marsh development. We deduce that lower fractions of labile carbon in deeper soils reflect long-term degradation, which underscores the notion that high recent rates of carbon accumulation are generally not sustained over centuries and millennia. Our research demonstrates the importance of identifying various carbon fractions in understanding carbon burial in freshwater marsh soils, and informing marsh conservation.

Hosted file

`956661_0_art_file_10721459_rq8z9c.docx` available at https://authorea.com/users/544872/articles/626884-drivers-of-high-rates-of-carbon-burial-in-a-riverine-influenced-freshwater-marsh-in-the-lake-erie-watershed-of-southern-ontario-canada

Hosted file

`956661_0_supp_10744273_rqnpb9.docx` available at https://authorea.com/users/544872/articles/626884-drivers-of-high-rates-of-carbon-burial-in-a-riverine-influenced-freshwater-marsh-in-the-lake-erie-watershed-of-southern-ontario-canada

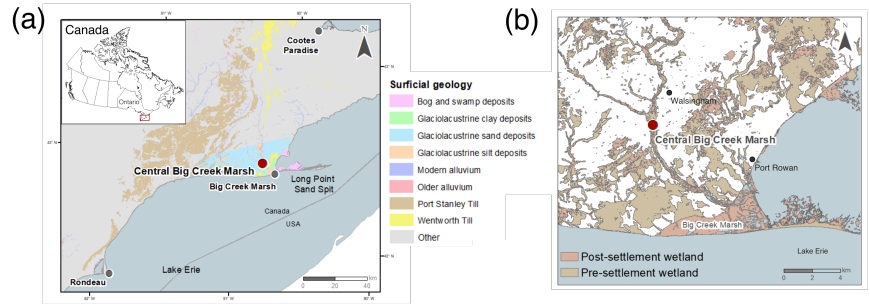

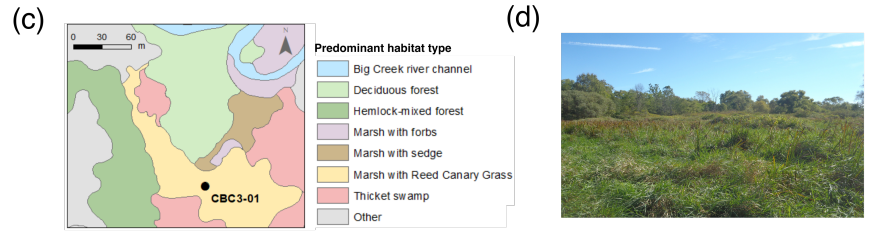

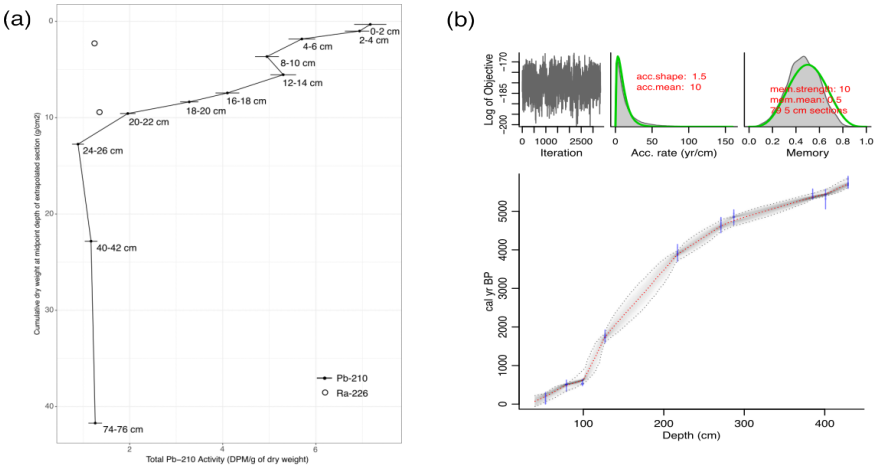

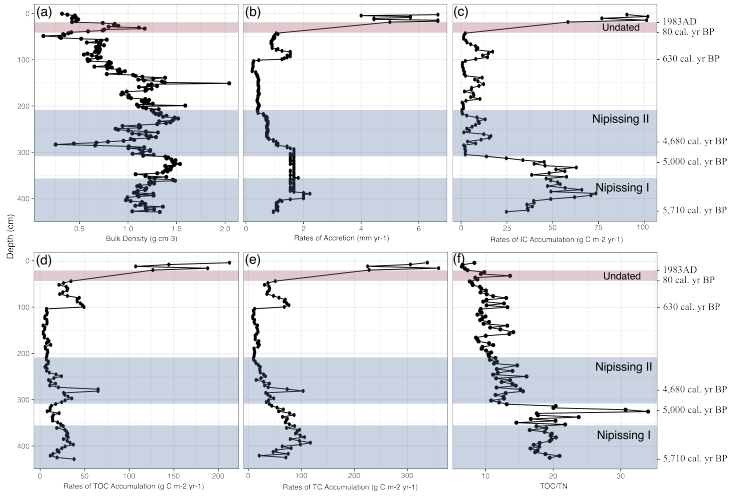

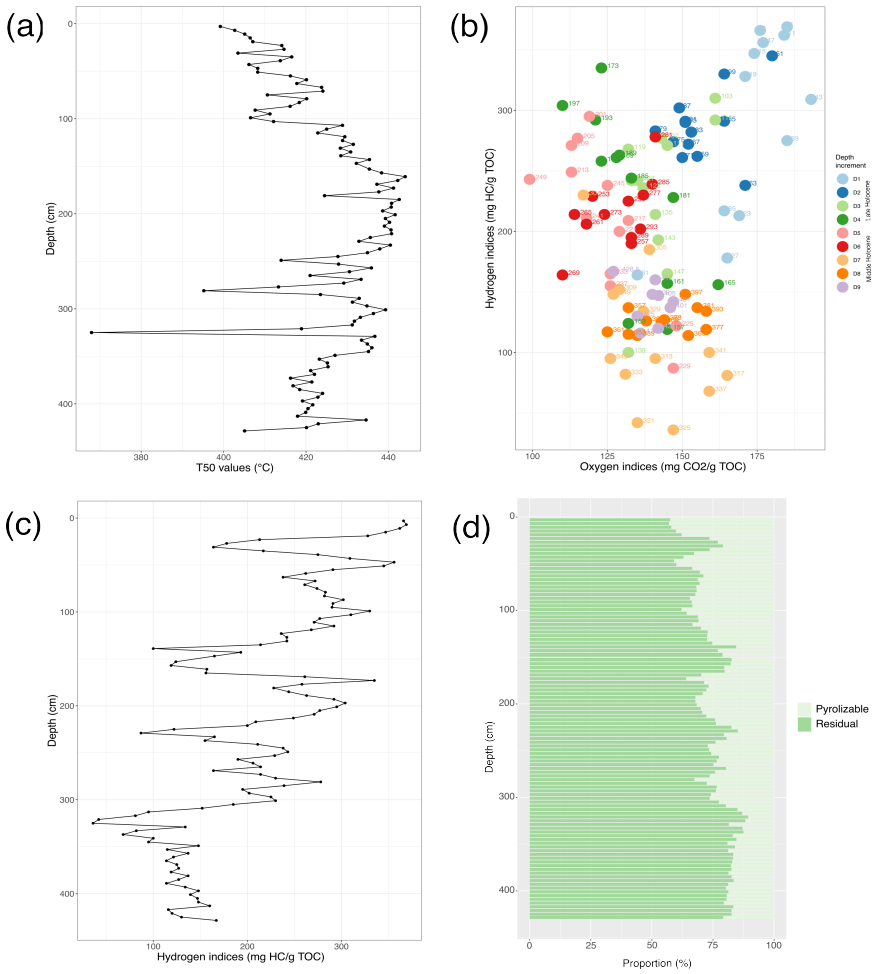

Drivers of high rates of carbon burial in a riverine-influenced freshwater marsh in the Lake Erie watershed of southern Ontario, Canada

Amanda L. Loder [1], Adam Gillespie[2], Omid Haeri Ardakani[3], Sarah A. Finkelstein[4]

[1] Department of Geography & Planning, University of Toronto, Ontario, Canada, M5S 3G3

[2] School of Environmental Sciences, University of Guelph, Ontario, Canada

[3] Natural Resources Canada, Geological Survey of Canada, Calgary, Alberta, Canada

[4] Department of Earth Sciences, University of Toronto, Ontario, Canada

* Corresponding Author:

Amanda L. Loder

Geography & Planning, University of Toronto

100 St. George Street

Toronto, ON M5S 3G3

Canada

902 229 2990

amanda.loder@mail.utoronto.ca

https://orcid.org/0000-0003-0222-6516

Abstract

Freshwater marshes are prevalent and important stores of carbon. They bury carbon in deeper soils, although reported rates of carbon accumulation are significantly higher over recent (decadal) versus longer (centennial and millennial) timescales. Intrinsic organic matter degradation, long-term climatic and ecological changes, and recent anthropogenic impacts on sediment fluxes and organic matter production may have a role in explaining this discrepancy, yet remain poorly understood for freshwater marshes. We collected a 4-m core from a riverine-influenced marsh in the watershed of Big Creek which drains into Lake Erie in southern Ontario, Canada, and conducted radiometric dating, elemental analyses, and programmed pyrolysis for organic matter characterization. Over the past 5,710 calibrated years, burial of organic (on average 26 ± 34 g C m^{-2} yr^{-1}) and inorganic (22 ± 25 g C m^{-2} yr^{-1}) carbon fractions has resulted in high rates of carbon accumulation. We found that elevated recent rates of organic carbon accumulation are driven by fractions that have low thermal stability and are predominantly from aquatic sources. This type of organic carbon is buried intermittently in deeper marsh sediments and corresponds to major hydro-fluvial events (e.g., Nipissing highstands), which coincide with regional marsh development. We deduce that lower fractions of labile carbon in deeper soils reflect long-term degradation, which underscores the notion that high recent rates of carbon accumulation are generally not sustained over centuries and millennia. Our research demonstrates the importance of identifying various carbon fractions in understanding carbon burial in freshwater marsh soils, and informing marsh conservation.

Data Availability Statement

Data from this research will be made available at https://doi.org/10.6084/m9.figshare.19326227 once the manuscript is published.

Supporting Information

Supporting Information may be found in the online version of this article.

Author Contributions

ALL and SAF designed the study and carried out field work. ALL prepared samples, carried out laboratory analyses and assembled the datasets; OHA conducted programmed pyrolysis. ALL and SAF analyzed and interpreted data from age-depth model, loss-on-ignition and elemental analyses; AG and OHA analyzed and interpreted data from programmed pyrolysis. ALL prepared the manuscript; all authors reviewed the results, discussed the interpretations and revised the manuscript.

Plain language summary

Freshwater marshes soils can contain considerable amounts of carbon stored several meters deep. Analyses spanning the entire length of freshwater marsh soil profiles are uncommon and the functions that enable them to sequester carbon and provide a means of mitigation against global warming are poorly understood. We conducted geochemical analyses on a 4-m soil core from a riverine freshwater marsh in a Lake Erie watershed to quantify and characterize carbon stores in marsh soils and understand why rates of carbon burial appear markedly higher over recent decades in comparison to past centuries and millennia. We found that organic and inorganic carbon are buried at high rates, but easily degradable organic matter predominates at the surface

and is lost in deeper soils, which in part explains the apparent slower rates of long-term carbon accumulation measured in marsh cores. Nonetheless, major fluctuations in Lake Erie water levels dating back thousands of years have enhanced burial and preservation of carbon in marsh soils. We demonstrate the importance in examining long records that capture all carbon types and the implications of long-term decay of organic carbon. These types of analyses are critical in assessing the role of marshes as a natural climate solution.

Key words: Wetland; carbon sequestration; programmed pyrolysis; paleoecology; Nipissing rise; Holocene; Laurentian Great Lakes

1 Introduction

There is a need to improve carbon flux quantifications in the terrestrial biosphere because of their potential to mitigate or amplify anthropogenic-induced global warming; yet, land fluxes of carbon remain challenging to quantify due to high spatial and temporal variability (Archer, 2010; Ciais et al., 2014). In recent years, there has been a growing interest in the role of wetlands in the global carbon cycle. Wetlands are recognized as a significant carbon pool with potential to take up or release enough carbon to influence the global climate, while simultaneously supporting bio- and cultural diversity (Heimann & Reichmann, 2008; Petrescu et al., 2015; Dinerstein et al., 2020; Pyke et al., 2021). Carbon stocks in wetlands are predominantly contained in wetland soils, where partially-decayed biomass can be buried and stored for centuries and millennia (Kayranli et al., 2010; Yu et al., 2010; Kolka et al., 2018). Wetland conservation and restoration have been identified as potential natural climate solutions in the temperate region where wetland alteration is widespread (e.g., Drever et al., 2021); however, carbon stocks for the entire soil profile of various temperate wetlands remain poorly constrained (Kolka et al., 2018).

Freshwater marshes are a broad group of wetlands characterized by emergent, soft-stemmed herbaceous vegetation with the capacity to adapt to and tolerate saturated and dynamic conditions. These marshes are especially prevalent in the temperate region yet are highly susceptible to drainage and conversion for agricultural use (Zoltai, 1988; Reddy & Delaune, 2008; Mitsch & Gosselink, 2015). While freshwater marsh soils are generally considered mineral-based with low organic matter contents, freshwater marshes support significant organic carbon burial over decades, centuries and millennia, and can contain peat horizons (Loder & Finkelstein, 2020). In temperate North America, estimates of short-term (past 50–100 years) apparent rates of carbon accumulation in freshwater marshes are on average 155 g C m^{-2} yr^{-1}; far

fewer measurements of long-term (over centuries and/or millennia) rates are reported (Loder & Finkelstein, 2020). Due to this paucity of data, rates of long-term carbon accumulation are poorly constrained, and it is not well known how much carbon is buried and preserved over longer time scales in freshwater marsh soils.

Available data suggest that recent rates are significantly higher than long-term apparent rates of carbon accumulation in freshwater marsh soils. Although this difference is not well characterized in freshwater marshes, it has been more thoroughly studied in coastal wetlands and northern peatlands. High recent rates of carbon accumulation in coastal wetlands are often attributed to accelerating relative sea level rise (e.g., McTigue et al., 2019; Rogers et al., 2019), while other work suggests that factors related to human activities (including eutrophication, landscape alteration and invasive species) may perturb carbon balances and elevate recent rates (Bansal et al., 2019; Spivak et al., 2019; Peteet et al., 2020; Gailis et al., 2021). In northern peatlands, it is well established that past apparent rates of carbon accumulation are lower than recent rates because the former are measured on samples that have already undergone some degree of long-term decay (e.g., Clymo, 1984), although extrinsic factors (e.g., climatic changes, wildfire, hydrological change, human activity) can influence both rates (e.g., Packalen & Finkelstein, 2014; Marrs et al., 2019; Young et al., 2019). For freshwater marshes, investigation is required to determine how intrinsic (e.g., organic matter lability, long-term decay) and extrinsic factors in temperate landscapes affect recent versus long-term rates of carbon; this will help ensure that rates are accurately captured for estimates of the strengths of natural carbon sinks. Otherwise, making the assumption that recent rates are sustained over the long-term may result in the overestimation of the strength of these natural sinks and lead to negative outcomes

including overly generous emission offsets (Bridgham et al., 2014; Neubauer, 2014; Young et al., 2019).

Freshwater marshes bury and preserve autochthonous (*in situ*) and allochthonous organic carbon derived from the surrounding watershed due to their variable hydrological regimes (Bridgham et al., 2006; Drexler, 2011; Van de Broek et al., 2018). Consequently, carbon accounting in freshwater marshes has additional complexities, as there are multiple pathways by from which carbon is derived and deposited over time, and the carbon stock in marsh soils may not solely reflect *in situ* production of organic matter (Bridgham et al., 2006). Furthermore, freshwater marsh soils contain both organic and inorganic carbon (Mitsch & Gosselink, 2015). Although inorganic carbon fractions can be negligible and are infrequently examined, carbonate burial may be significant in ecosystems where allochthonous sources of carbonate (e.g., coral reefs, lithogenic sources) are present (Martin, 2017; Saderne et al., 2019) and thus needs to be differentiated from organic carbon burial for carbon accounting purposes.

This study focusses on long-term apparent rates of carbon accumulation since the formation of a riverine-influenced freshwater marsh which is mineral-based, proximal to intensive anthropogenic land-use activities and in a temperate region with a history of large-scale hydro-climatic change associated with the Laurentian Great Lakes. The objectives of our study are to: 1) characterize organic matter and quantify carbon fractions since the Middle Holocene in a freshwater marsh core; 2) track long-term apparent rates (hereafter long-term rates) of carbon accumulation during the Holocene, when marsh formation in temperate North America was initiated (e.g., Finkelstein & Davis, 2006; Rippke et al., 2010; Drexler, 2011), in relation to local and regional hydroclimatic change; and 3) evaluate factors leading to elevated recent versus long-term rates of carbon accumulation. The geochemical paleorecord allows us to evaluate the

impacts of both intrinsic and extrinsic factors on marsh sediment and carbon accumulation. To address these questions, we use radiometric dating, elemental analyses, programmed pyrolysis and carbon to nitrogen (C/N) ratios to examine how organic matter composition reflected hydroclimatic change and rates of carbon burial in the paleorecord, and to quantify organic and inorganic fractions that make up the total carbon stock in freshwater marsh soils. Programmed pyrolysis was selected as it measures the thermal stability of soil organic matter in marsh soils, allowing direct evaluation of the role of organic matter lability in differentiating recent versus long-term rates of carbon accumulation.

2 Methods

2.1 Study site

Central Big Creek Marsh (42.65° N, 80.54° W) is situated on modern alluvial deposits on the floodplain of Big Creek in Norfolk County, southern Ontario (Figure 1). Norfolk County is on the traditional lands of the Attawandaron, Haudenosaunee and the Anishinaabe First Nations, and encompassed within the Treaty lands ('Between the Lakes Purchase') of the Mississaugas of the Credit. The site is located approximately 8 km from the Lake Erie shoreline and about 2 m above the mean annual level of Lake Erie (~174 m asl; NOAA, 2022). At present day, the site supports predominantly monotypic stands of Reed Canary Grass (*Phalaris arundinacea*); other marsh plants include *Schoenoplectus tabernaemontani, Sparganium eurycorpum* and *Nuphar lutea,* and *Lemna spp.* in pools of standing water. Surrounding ecotypes encompass thicket swamp and upland Carolinian forest (Figure 1). The climate is temperate with daily mean temperatures of 21.1 °C in July and minus 5.4 °C in January, and annual precipitation of 1036 mm (Delhi, ON, 1981–2010; Environment and Climate Change Canada, 2021). The bedrock in the Big Creek watershed is comprised of limestone carbonates, overlain by modern and older

168 alluvium around the Big Creek channel, and by carbonate-rich till and glaciolacustrine deposits
169 of clay, sand, and silt in other parts of the watershed (Barnett, 1993).
170 Around Lake Erie, long-term fluctuations of lake levels related to differential glacial
171 isostatic adjustment have had a strong influence on wetland development over the post-glacial
172 (Coakley & Lewis, 1985; Pengelly et al., 1997; Bunting and Warner, 1998; Finkelstein & Davis,
173 2006). During the Middle Holocene, a two-pulsed event related to outlet incision and drainage
174 from the upper to lower Great Lakes caused water levels in Lake Erie to rapidly rise and decline
175 by several meters (termed the Nipissing highstands; Coakley & Lewis, 1985; Finkelstein et al.,
176 2006). The first of these highstands known as Nipissing I resulted in a rapid increase in water
177 level ~5,960 cal. yr BP, followed by a decline ~5,200 cal. yr BP. Nipissing II was a subsequent
178 increase in water level which reached a maximum ~4,480 cal. yr BP and dropped ~3,770 cal. yr
179 BP (Lewis et al., 2012). Water levels in Lake Erie have since fluctuated at a lower magnitude
180 (i.e., 1–2 m) over the past 3,000 cal. yr BP (Coakley & Lewis, 1985; Pengelly et al., 1997;
181 Finkelstein & Davis, 2006; Lewis et al., 2012). Periods of high and low water stands in Lake
182 Erie during and following the Nipissing events affected water levels in coastal marshes
183 (Finkelstein & Davis, 2006), and could have caused inundation and water table levels to fluctuate
184 in low-lying riverine-influenced marshes. Thus, these events had potential to promote or reduce
185 local production and preservation of organic matter, as well as inputs of minerogenic materials,
186 and to ultimately affect sedimentation and carbon accumulation in marsh soils (Van de Broek et
187 al., 2016; Van de Broek et al., 2018).
188 Based on soil maps, topographic, hydrological data, and land cover information, marsh
189 and swamp habitat were extensive in Norfolk County prior to European settlement and 82% of
190 wetlands have since been lost in this region (Snell, 1987; Ducks Unlimited Canada, 2010; Byun

et al., 2018; Figure 1). Widespread marshland had established across the Big Creek watershed due to low-lying topography, the low permeability of glaciolacustrine deposits and riverine influence (Byun et al., 2018). Europeans arrived in Norfolk County during the mid-17th century, and the first significant period of European settlement took place between 1790 and 1820 AD (Chapman & Putnam, 1984). Shortly after, large-scale deforestation, drainage and intensive landscape alterations occurred primarily in support of agricultural development and continued into the 20th century, resulting in massive increases in rates of erosion (Bunting et al., 1997; Riley, 2013).

2.2 Sampling

A 430-cm sediment core (CBC3-01) was recovered from Central Big Creek Marsh in October 2019 using a Russian peat corer of barrel length 50 cm (Eijkelkamp Soil and Water, Giesbeek, the Netherlands) to minimize compaction. Like other minerogenic marsh cores (e.g., Drexler et al., 2009; Peteet et al., 2020), we did not observe sediment compaction upon examining the soil cores. Standing water was not present at the time of sampling. Core samples were stored in plastic split tubes, kept in the dark and refrigerated at 4 °C in the University of Toronto Paleoecology Laboratory until sub-sectioning began. The CBC3-01 sediment core was subsampled at contiguous 2-cm intervals. Samples of 6.28 cm^3 from every subsection were dried and weighed to constant mass for bulk density measurements.

2.3 Radiocarbon and ^{210}Pb dating

Radiocarbon dates were obtained from wood samples (*N*=9) and plant macrofossils (*N*=1; Table 1). Samples were washed with reverse-osmosis water, dried at ~60 °C to constant mass, and sent to the A.E. Lalonde AMS Laboratory (Ottawa, Ontario, Canada) for radiocarbon dating via Accelerator Mass Spectrometry (AMS). An age-depth model was developed for CBC3-01 at

1-cm increments using the rbacon package (Bayesian age-depth modelling) in R (Version 3.6.3; Goring et al., 2012) to infer rates of vertical accretion (hereafter rates of accretion) accounting for both inorganic and organic sediments. Ages were calibrated using OxCal 4.4 (Bronk Ramsey, 2009) with the IntCal20 calibration curve (Reimer et al., 2020), and are expressed as calendar years before present (hereafter cal. yr BP) in relation to 1950 AD.

Contiguous sediment samples were analyzed for lead-210 (^{210}Pb) activities in more recently deposited sediments. Dried material (~0.5 g) was allocated from each 2-cm subsection of the top 0–30 cm of CBC3-01 for supported ^{210}Pb activities (i.e., background levels) by examining radium-226 (^{226}Ra), and for unsupported ^{210}Pb activities by subtracting the supported ^{210}Pb activities from the total ^{210}Pb activities. These samples were ground to fine powder using a ball mill and sent to Flett Research Ltd. (Winnipeg, Manitoba, Canada) for analysis of ^{210}Pb activity. Total ^{210}Pb activity was measured via polonium-210 by alpha spectrometry and supported ^{210}Pb activity (in secular equilibrium with Ra-226) was determined by radon-222 emanation.

2.4 Elemental analyses and programmed pyrolysis

Dried material from every second 2-cm increment of CBC3-01 was ground to fine powder using a ball mill for elemental analyses and programmed pyrolysis. The first allocation was analyzed for total carbon and total nitrogen (TN; ~400 mg ground sample) using a LECO CHN628 elemental analyzer in the Radiochronology Laboratory at the Centre for Northern Studies at Université Laval.

The second allocation was used for programmed pyrolysis (~70 mg ground sample) using HAWK TOC analyzer at the Geological Survey of Canada (Calgary, Alberta, Canada) to measure total organic carbon (TOC) content and inorganic carbon (in carbonates), and to

characterize organic matter type. Programmed pyrolysis was originally developed for petroleum exploration (LaFargue et al., 1998; Behar et al., 2001), but has started to be applied to surficial soils for characterizing organic matter, discerning lability and differentiating organic versus inorganic carbon fractions (Carrie et al., 2012; Hare et al., 2014; Galloway et al., 2018; Kemp et al., 2019). More specifically, programmed pyrolysis measures different organic matter fractions, and their thermal stability and potential for decomposition, making it an ideal method to evaluate the effects of organic carbon lability on recent- versus long-term rates of carbon burial in freshwater marsh soils (Soucémarianadin et al., 2020; Kanari et al., 2022; Zhang et al., 2023). Spectroscopic methodologies that characterize wetland soil organic matter such as Fourier-Transform Infrared Spectroscopy (FTIR) identify chemical bonds of organic carbon, but do not directly quantify labile versus recalcitrant organic carbon, or inorganic carbon fractions. During pyrolysis, soil samples were subjected to iso-temperature heat at 300 °C for three minutes to determine the total free (labile) hydrocarbon released (S1 fraction). The temperature was subsequently ramped up to 650 °C at 25 °C per minute to release, through thermal cracking, thermal-stable hydrocarbons and the oxygen contained in pyrolizable kerogen (S2 fraction, mg HC/g sediment, and S3 fraction, mg CO_2/g sediment, respectively). Samples were then automatically transferred to the oxidation oven and heated from 300 °C to 850 °C with the heating rate of 20 °C per minute to measure the residual inert organic carbon (S4 fraction, mg CO and CO_2/g sediment and residual carbon, weight %) and the mineral (inorganic) carbon fraction. Total organic carbon is quantified as the sum of the total quantity of organic matter released during the pyrolysis and the oxidation steps. The hydrogen index (HI) is the ratio of S2 to TOC and is proportional to H/C, while the oxygen index (OI) is calculated by normalizing the quantity of the pyrolizable CO_2 (S3) to TOC and is proportional to the elemental O/C ratio of

organic matter (Lafargue et al., 1998; Behar et al., 2001). The thermal stability of organic matter in the soil samples was examined by identifying the temperatures at which half of the pyrolizable hydrocarbon (S1 and S2) was released during pyrolysis (hereafter T50 measurements; Gregorich et al., 2015). Finally, ratios of 'generative' (S1, S2 and S3) and 'non-generative' (S4) organic carbon in relation to TOC were calculated to estimate the proportions of pyrolizable versus residual fractions of organic carbon down core in CBC3-01.

To verify our organic and inorganic carbon measurements from programmed pyrolysis, we allocated a portion of unground material from every second 2-cm increment of CBC3-01 for standard loss-on-ignition (LOI) analyses (see Supporting Information for more on methods and for results). Furthermore, we allocated an additional ~150–200 mg of ground material from 13 increments from CBC3-01 to measure inorganic carbon using an SSM-5000A Solid Sample Combustion Unit in a Shimadzu TOC-L Analyzer at the Analytical Laboratory for Environmental Science Research and Training (ANALEST) at the University of Toronto (see Appendix A for results). Carbon to nitrogen ratios have been used in lake and wetland ecosystems to determine the extent to which aquatic ($C/N < 10$; attributed to algae and aquatic plants that are enriched in lipids and proteins) and/or terrestrial ($C/N > 20$; attributed to terrestrial and vascular plants that are enriched in lignin and cellulose) production contribute to organic matter preserved in bulk sediments in paleoenvironments (Meyers & Teranes, 2001; Kim, 2003; Khan et al., 2015). Given the significance of inorganic carbon in the sediments of CBC3-01, we calculated C/N values using the ratio of TOC to TN (hereafter TOC/TN) fractions to examine whether the organic matter was derived from aquatic versus terrestrial environments.

Organic, inorganic and total carbon densities were calculated for every 2-cm increment using the bulk density measurements and were used in conjunction with rates of accretion to

calculate rates of carbon accumulation (e.g., Bao et al., 2011; Drexler, 2011; Jones et al., 2014; Delaune et al., 2018). Soil core data from this manuscript is available at Loder et al. (2022).

3 Results

3.1 Chronology and rates of accretion

The chronology of CBC3-01 was obtained from the unsupported ^{210}Pb profile (0–20 cm depth; Figure 2(a)) and a model of ^{14}C dates (40–429 cm depth; Figure 2(b)). We developed the rbacon model for CBC3-01 solely based on the radiocarbon dates and applied the model between 40 and 429 cm depth. In the top-of-core section, total ^{210}Pb activity decreases exponentially with depth from 0 cm down to 20 cm in CBC3-01. In this same interval, dry bulk density measurements are <0.50 g cm^{-3}, but rapidly increase below 20 cm to a high of 1.17 g cm^{-3} at 33 cm and drop below 0.50 cm^{-3} at 41 cm (Figure 3). Radium-226 measurements were 1.22 and 1.29 DPM/g at 6–8 cm and 20–22 cm, respectively, both of which are lower than total ^{210}Pb activities between 0–22 cm yet higher than the total ^{210}Pb activity at 22–24 cm. The total ^{210}Pb activities at 40–42 cm and 74–76 cm are not significantly different than the ^{226}Ra activities and indicate background (supported) levels.

We infer that core CBC3-01 does not contain a continuous profile of 110+ years of accumulated sediments needed to build an accurate ^{210}Pb inventory, and that sediment accumulation processes between 20–40 cm are uncertain and were likely affected by truncation and/or atypical imports of material older than 110 years. However, given the sufficiently linear trend in unsupported ^{210}Pb activities between 0–20 cm, we can approximate sediments at 20 cm depth to be less than 2 half-lives of ^{210}Pb (45 years). We use a constant rate of supply model (calibrated against the linear regression model) to apply ^{210}Pb age modelling to the top 20 cm of CBC3-01. We consider 0–20 cm as the datable, post-settlement section in CBC3-01 and leave

20–40 cm undated. Dates between 40–52 cm are extrapolated from the rbacon model and thus should be interpreted with caution (Figure 2).

Basal sediments in CBC3-01 date to 5,710 cal. yr BP (Table 1) and correspond to Nipissing I of Lake Erie associated with widespread wetland initiation and marsh establishment in coastal zones of the lower Great Lakes (Finkelstein and Davis, 2006; Lewis et al., 2012). Rates of accretion in Central Big Creek Marsh ranged between 0.2–6.7 mm yr^{-1} (Figure 3), which are similar to rates in other local lacustrine-influenced marshes located on the shores of the lower Great Lakes including Cootes Paradise (1.0–7.1 mm yr^{-1}; Finkelstein et al., 2005) and Lower Big Creek Marsh (1.8 mm yr^{-1}; Bunting et al., 1997; Figure 1). Between 5,710–4,640 cal. yr BP rates of accretion at CBC3-01 were greater than 1.0 mm yr^{-1} but subsequently dropped and steadily declined down to 0.2 mm yr^{-1} by 1,670 cal. yr BP. Rates of accretion sharply rose after 630 cal. yr BP and varied between 0.9 and 1.5 mm yr^{-1} until ~80 cal. yr BP. These rates increased several-fold in the most recent part of the record, with the highest values (up to 6.7 mm yr^{-1}) between 1983 and 2019 AD.

3.2 Rates of carbon accumulation

Organic carbon burial has been occurring at Central Big Creek Marsh since its formation 5,710 cal. yr BP with an average (± standard deviation) long-term rate of organic carbon accumulation of 26 ± 34 g C m^{-2} yr^{-1}. Rates of inorganic carbon accumulation were notably high following initiation, but declined after 4,970 cal. year BP.

High rates of organic carbon accumulation were sustained during the Nipissing highstands (Figure 3). During Nipissing I, rates of organic carbon accumulation in Central Big Creek Marsh reached 37 g C m^{-2} yr^{-1} and declined following the highstand. At the time of Nipissing II, a short-term peak in organic carbon burial (65 g C m^{-2} yr^{-1}) occurred around 4,680

329 cal. yr BP, which coincided with the approximate time of initiation of marshes in adjacent
330 coastal areas of Lake Erie (e.g., Finkelstein & Davis, 2006). Following Nipissing II, rates of
331 organic carbon accumulation dropped and remained <10 g C m^{-2} yr^{-1} between 4,160 cal. yr BP
332 and 630 cal. yr BP.

333 Rates of organic, inorganic, and total carbon accumulation increased around 630 cal. yr
334 BP and remained elevated until present day. However, rates of organic carbon accumulation
335 were high and variable between 1983–2019 AD and coincided with maximum rates of sediment
336 accretion. During this 36-year period (0–20 cm depth), rates of total carbon accumulation were
337 between 225 and 359 g C m^{-2} yr^{-1}, which comprised both organic and inorganic fractions of
338 carbon; these rates are 1–2 orders of magnitude higher than any recorded during the Holocene in
339 this record (Figure 3).

340 **3.3 TOC/TN ratios**

341 Between 5,710–4,930 cal. yr BP, TOC/TN ratios varied between 15 and 24, except for an
342 increase to 34 at 5,000 cal. yr BP during the lowstand after Nipissing I (Figure 3). These are the
343 highest TOC/TN values in the CBC3-01 paleorecord and are driven by low TN contents. Since
344 this lowstand and through the Late Holocene, TOC/TN ratios have fluctuated between 6 and 16.
345 Values of TOC/TN in CBC3-01 are predominantly <10 in sediments deposited over the past 400
346 cal. yr BP.

347 **3.4 Thermal stability of carbon fractions**

348 The S1, S2 and S3 values derived from programmed pyrolysis and TOC content follow
349 each other closely in CBC3-01 (see Figure S6 in Supporting Information). Samples are
350 predominantly comprised of S2 thermal-stable hydrocarbons (range of 0.13–37.07 mg HC/g soil;
351 mean [± standard deviation] equal to 6.73 ± 7.64 mg HC/g soil), with smaller proportions of S3

352 pyrolizable organic matter (range of 0.51–18.88 mg CO_2/g soil; mean equal to 3.95 ± 3.87 mg
353 CO_2/g soil) and more minor proportions of S1 labile hydrocarbons (range of 0.02–5.46 mg HC/g
354 soil; mean equal to 0.79 ± 1.13 mg HC/g soil).
355 Temperature measurements of T50 generally increase down core in CBC3-01 (Figure 4).
356 Between 5,710–5,150 cal. yr BP, T50 values ranged from 405°C (at the basal sediments) to
357 435°C. However, T50 values subsequently became highly variable, with temperatures as low as
358 368°C (at 325 cm) and 395°C (at 281 cm), until 2,300 cal. yr BP. The rapid decline in T50
359 values at 281 cm and subsequent up-core variability matches the variability in S1 values (Figure
360 S6). Overall, T50 values were generally lowest (between 399–424°C) in sediments deposited
361 over the past 630 cal. yr BP.
362 Hydrogen and oxygen indices range between 36–369 mg HC/g TOC and 99–193 mg
363 CO_2/g TOC, respectively, in CBC3-01 (Figure 4). Between 5,710–4,900 cal. yr BP (below 300
364 cm depth), HI values were typically low (<150 mg HC/g TOC) while OI indices ranged between
365 125–165 mg CO_2/g TOC. Between 4,900–2,270 cal. yr BP, OI values were generally lower than
366 in the Middle Holocene soils, while HI values were generally higher through the Late Holocene
367 (top 200 cm of CBC3-01). Hydrogen indices gradually increased between 2,280–630 cal. yr BP
368 and thus decrease with depth between 100–150 cm. Since 630 cal. yr BP, both HI and OI values
369 were elevated. Recently-deposited sediments in the top 100 cm of CBC3-01 comprise some of
370 the highest HI and OI values up to 369 and 193, respectively, except for disturbed samples
371 between 20–40 cm which have the lowest HI values.
372 Proportions of residual versus pyrolizable organic carbon vary down core in CBC3-01
373 but are predominated by the residual fraction (between 57–89 %; Figure 4). Following marsh
374 initiation and during Nipissing I, the residual fraction of organic carbon was predominantly >80

%, but began to decline (while the pyrolizable fraction simultaneously increased) during Nipissing II and reached a minimum of 68 %. Proportions of pyrolizable organic carbon have generally been higher (up to 43 %) since 630 cal yr BP, with lower values in the undated sediments between ~80 cal. yr BP and 1983 AD.

4 Discussion

4.1 Composition and origins of carbon stocks

Carbon stocks in whole-profile soils of freshwater marshes are rarely considered in soil carbon inventories to date due to a lack of data. In this study, we demonstrate that non-tidal freshwater marshes bury carbon at high rates on decadal, centennial and millennial scales. These marshes have potential to stabilize several meters of carbon in their soils over thousands of years when connected to a large network of freshwater ecosystems (e.g., the Great Lakes) and when situated on a riverine floodplain where deposition rates are high. Furthermore, we show that while long-term rates of carbon accumulation were elevated during major water level rises in Lake Erie, recent rates of carbon accumulation are several-fold higher than long-term rates calculated through the Middle and Late Holocene.

Organic carbon stores in Central Big Creek Marsh are predominantly comprised of a 'residual' or inert fraction which is resistant to pyrolysis. When transported through the sedimentary environment, the residual fraction is often coupled with or bound to the mineral fraction in fluvial sediments, and consequently is physically stable and protected from further biological degradation (Mudd et al., 2009; Van de Broek et al., 2018; Repasch et al., 2021). Because the residual fraction is deposited in downstream lowlands (Repasch et al., 2021) and is suited for preservation over hundreds to thousands of years, we deduce that this fraction has a strong, positive influence on long-term rates of organic carbon accumulation in riverine-

influenced freshwater marshes. The proportion of pyrolizable organic carbon relative to the residual fraction of organic carbon decreases with depth throughout the core, suggesting that organic carbon deposits in surface sediments are less thermally stable than deeper deposits due to organic matter breakdown via microbial processes. We therefore conclude that recent accumulations of organic carbon in freshwater marshes are susceptible to and undergo biological degradation, and that a more resistant fraction remains with increasing depth. This corroborates the relationships observed between increased thermal stability and the loss of labile organic matter in other environments (e.g., arable versus fallow agricultural fields, surface versus buried organic matter in Arctic hummocks; Gillespie et al., 2014; Gregorich et al., 2015). Even in the absence of human impacts, short-term rates are very likely to be elevated relative to longer-term rates.

Our analysis shows that labile organic carbon stores are not only present in recent deposits, but also in distinct layers at depth in freshwater marsh soils. During the Middle to Late Holocene transition, layers of organic carbon with low thermal stabilities were buried intermittently among more stable layers of organic carbon in deeper soils, notably at 325 cm (5,000 cal. yr BP), 281 cm (4,710 cal. yr BP) and 249 cm (4,320 cal. yr BP) depths (Figure 4). The latter two depths are also characterized by high levels of the most thermolabile fraction of organic carbon (S1 and S2), demonstrating that pockets of undecomposed and highly labile material are preserved in the marsh profile. Deeper soils, thus, cannot be discounted in carbon inventories of freshwater marshes given their potential to comprise significant organic carbon stocks that can readily degrade if disturbed (i.e., drained) and exposed to oxygen.

Ratios of TOC/TN measured in bulk sediments can be used to differentiate those that contain predominantly aquatic- versus terrestrially-derived organic matter because aquatic

organic matter comprises N-rich proteins and H-rich lipids, and terrestrial organisms typically contain cellulose-rich structural tissue (Meyers & Teranes, 2001; Khan et al., 2015). Using TOC/TN values, we found that recently-deposited sediments comprise a significant proportion of labile organic matter with low TOC/TN values which was likely produced by aquatic organisms (Meyers and Teranes, 2001; Carrie et al., 2012; Khan et al., 2015). This result may additionally reflect added nutrient influxes due to intensive agricultural activity in the watershed and/or the presence of invasive *Phalaris arundinacea* in Central Big Creek Marsh. Nevertheless, organic matter characterizations through the paleorecord suggest that Central Big Creek Marsh accumulated higher proportions of organic matter derived from aquatic sources throughout the Late Holocene. Conversely, organic matter stores from the Middle Holocene differ in composition and show comparatively higher TOC/TN values. This organic matter was likely derived primarily from terrestrial sources (Figure 4). Terrestrial organic matter comprises predominantly lignin and cellulose which are more resistant to decomposition than lipids and proteins in autochthonous organic matter (Reddy & Delaune, 2008; Carrie et al., 2012). Therefore, these organic fractions that were deposited in Central Big Creek Marsh during the Middle Holocene may have good potential for long-term preservation in undisturbed marsh environments, and require consideration when discerning differences in rates of organic carbon accumulation throughout the paleorecord.

Most studies rely only on quantifications of organic carbon or find that the inorganic carbon fraction is negligible in marsh soil samples (Loder & Finkelstein, 2020). In our study, we found that both organic and inorganic fractions of carbon drive elevated rates of total carbon accumulation in this freshwater marsh. The Big Creek watershed is underlain by glacial sediments from the Wentworth and Port Stanley tills (Figure 1), which are rich in carbonates

(mean contents of 36 % and 37.0 %, respectively). These tills are further underlain by limestone associated with the Dundee Formation (Barnett, 1993; Lewis et al., 2012). Through erosional processes and/or water infiltration, these deposits are the major source of carbonates in the Big Creek watershed and contribute to elevated carbonate burial in Central Big Creek Marsh. Coastal ecosystems have recently been recognized for their potential to enhance carbon sequestration because local calcification processes and resultant carbon dioxide (CO_2) outputs are minimal, and marine-derived carbonates may be accrued from local lithogenic sources and modern coral reefs and undergo dissolution in coastal ecosystems (requiring the removal of CO_2; Martin, 2017; Saderne et al., 2019). More research is required to determine whether carbonate burial could enhance carbon sequestration in freshwater marshes through similar processes that have been identified in marine-influenced wetlands.

4.2 Implications of hydroclimatic events on carbon burial in wetlands

We found three major shifts in organic carbon composition and burial in the CBC3-01 paleorecord which coincided with past hydroclimatic events. The first occurred during the lowstand following Nipissing I (Figure 3) and is characterized by a marked increase in labile organic carbon and more terrestrially-derived organic carbon. Central Big Creek Marsh is situated 2 m above lake level at present day; based on glacial isostatic adjustment, the core top of CBC3-01 would have been about 0.5–1 m above lake level during the Middle Holocene (Lewis et al., 2012; Lewis et al., 2021). We conclude that the rise in Lake Erie water levels by several meters during Nipissing I caused inundation and elevated the water table at the CBC3-01 site, and ultimately triggered the formation of marshland. The lowering of lake water levels following Nipissing I likely reduced inundation and decreased water table levels, and may have resulted in

a decline in aquatic primary productivity which was compensated by an apparent increase in terrestrial production and inputs at Central Big Creek Marsh.

The second shift occurred at the time of Nipissing II (4,680 cal. yr BP; 277 cm depth), and is characterized by a marked increase in degradable organic carbon and rates of organic carbon accumulation. In this case, we conclude that the highstand of Nipissing II again caused inundation and increased the water table level at Central Big Creek Marsh. Coupled with warmer temperatures during the Middle Holocene in southern Ontario (Yu et al., 1996), these conditions would have stimulated aquatic primary productivity and organic carbon production. We also speculate that Central Big Creek Marsh served as a depositional environment during Nipissing II for rapid influxes of minerogenic sediments upon erosion and flooding from the Big Creek River channel. These minerogenic influxes can help bury and preserve *in situ* organic carbon by advecting organic matter to deeper sediment layers by rapid rates of accretion, and by reducing the time of exposure to diagenesis at the surface (Mudd et al., 2009; Van de Broek et al., 2016; Van de Broek et al., 2018; Kemp et al., 2019; Spivak et al., 2019).

Lastly, there was a prolonged period between 4,200–630 cal. yr BP (100–240 cm depth) during which rates of organic carbon accumulation were reduced and less variable. The decline in rates of accretion after Nipissing II coincided with the drop in water levels in Lake Erie (Lewis et al., 2012). In tidal marshes, the long-term accumulation of organic carbon in soils is controlled by sediment supply and is not solely related to local biomass production (Mudd et al., 2009; Van de Broek et al., 2016; Van de Broek et al., 2018). Thus, we speculate that water levels were lower and hydrological inputs reduced in Central Big Creek Marsh during this prolonged period, and that these conditions lead to higher rates of decomposition, and lower rates of organic carbon production and burial. In contrast, the Nipissing highstands in Lake Erie would

have enhanced bank erosion of marsh creeks and increased the sediment supply into Central Big Creek Marsh, thereby increasing the potential for burial and preservation of organic carbon (Yu et al., 2017; Van de Broek et al., 2018; Spivak et al., 2019; Repasch et al., 2021).

Like organic carbon, rates of inorganic carbon burial in Central Big Creek Marsh were also likely influenced by hydro-fluvial changes associated with the Nipissing highstands. Higher rates of inorganic carbon accumulation in the bottom 1-m of CBC3-01 are likely attributed to conditions during the Middle Holocene when temperatures were warmer and carbonate concentrations were higher in Lake Erie waters (Lewis et al., 2012). Upon the highstand of Nipissing I and formation of Central Big Creek Marsh, carbonate-rich waters likely inundated and precipitated *in situ* at CBC3-01 when water residence times were long enough. During Nipissing II, water that inundated Central Big Creek Marsh from Big Creek may have comprised fewer carbonates because the waters in the Lake Erie basin at that time had been transferred from the upper Great Lakes and more northern latitudes, were cooler in temperature and were diluted (Lewis et al., 2012). Alternatively, or in combination with the former, Lake Erie water and its carbonate supply may have been restricted at the mouth of the Big Creek river channel upon formation of the Long Point sand spit (Barnett et al., 1985), thereby reducing carbonate burial.

4.3 Recent versus long-term rates of carbon accumulation

Recent rates of organic and total carbon accumulation are high while long-term rates are generally slower in CBC3-01. Both recent and long-term rates can be comparable to rates in salt marshes and peatlands. This demonstrates that riverine-influenced freshwater marshes with high rates of vertical accretion and biomass production provide an important means for carbon storage. Although we largely attribute the marked difference between recent and long-term rates of organic carbon accumulation in Central Big Creek Marsh to losses of labile fractions over the

long-term, we suspect that other factors are contributing to this difference and require further investigation.

Hydroclimatic conditions associated with the Little Ice Age may have promoted higher rates of organic carbon accumulation. Around 630 cal. yr BP (100 cm depth), there was a notable increase in rates of accretion and carbon accumulation at Central Big Creek Marsh. Peat accumulation began around 650 cal. yr BP at Lower Big Creek Marsh (Bunting et al., 1997) and a cluster of short paleorecords from four separate sloughs have basal ages of approximately 700 cal. yr BP at the Rondeau Marshes (Finkelstein & Davis, 2006; Figure 1). All these events are attributed to higher water levels in eastern Lake Erie during the Little Ice Age when conditions were wetter in the eastern Great Lakes region of southern Ontario (Pengelly et al., 1997; Finkelstein & Davis, 2006), and collectively may have elevated water levels, rates of accretion and organic carbon accumulation in Central Big Creek Marsh.

In the more recent record, high and variable rates of accretion, and organic, inorganic and total carbon accumulation over the past 36 years collectively suggest that major landscape alterations affected rates of accretion and carbon accumulation. Even when accounting for different dating methods and errors covering different timespans, rates of alluvium accretion (associated with erosion) across North America are shown to have increased 10-fold post-European settlement due major landscape alterations and clearance for agriculture (Kemp et al., 2020). Because subsoils comprised of carbonates are increasingly exposed and eroded from landscapes that have experienced intensive farming, carbonate availability and deposition in proximate watersheds has been used as an indicator for tillage erosion (Papiernik et al., 2002; Zamanian et al., 2020). We suspect that elevated recent rates of accretion and inorganic carbon accumulation in Central Big Creek Marsh have resulted from increases in erosion and soil loss in

parts of the Big Creek watershed where intensive agricultural activity has taken place. Further research is required to discern the extent to which elevated recent rates of organic carbon accumulation are driven by the accumulation of labile fractions versus anthropogenic pressures in temperate wetlands.

Although differences in the timespan of measurements (e.g., ^{210}Pb versus ^{14}C dating techniques) have potential to cause discrepancies between short- versus long-term rates of accretion (Kemp et al., 2020), our geochemical analyses on core CBC-01 demonstrate continuous accretion through the dated sections of the paleorecord and elevated recent rates of accretion when dating errors are considered (as per Binford et al., 1990). Applying rates of mass accumulation instead of accretion when calculating rates of carbon accumulation can further increase the accuracy in rate measurements (Arias-Ortiz et al., 2018), and thus requires consideration in future research alongside the limitations in dating techniques when comparing short- versus long-term rates of carbon accumulation in freshwater marshes.

5 Conclusion

Non-tidal freshwater marshes have potential to bury and store considerable amounts of organic and inorganic carbon. We demonstrate that elevated rates of organic carbon accumulation in temperate freshwater marshes are episodic, yet can be as high as recent rates in salt marshes and as high as those in peatlands in the long-term when high rates of vertical accretion and local biomass production are sustained. These rates fluctuate in relation to major hydroclimatic events that caused water levels in the lower Great Lakes to fluctuate through the Holocene. Furthermore, they are vulnerable to anthropogenic-induced activities (e.g., land use, the presence of invasive species, nutrient loading) in the temperate region, which have potential to affect recent rates of organic carbon burial.

We show that organic carbon fractions in surface marsh soils are predominantly labile and will be subjected to decay in the ensuing centuries and millennia, thereby lowering long-term rates of organic carbon accumulation. Our finding that recent rates of organic carbon accumulation are attenuated over hundreds to thousands of years due to long-term decay corroborates findings in the coastal (tidal) wetland and peatland literature, and concerns that the extrapolation of recent rates over centuries and millennia leads to erroneous assumptions in wetland carbon budgets (Mudd et al., 2009; Bridgham et al., 2014; Young et al., 2019). Because of long-term decay and the various contents and properties of carbon fractions throughout the marsh paleorecord, it is critical to consider the entire profile and all carbon fractions when quantifying the climate mitigation potential of freshwater marsh soils and their role as a natural climate solution. Otherwise, high recent rates of organic carbon accumulation in freshwater marsh soils may provide a false sense of success in mediating the climate crisis if applied as carbon offsets over longer time scales.

Acknowledgements

We gratefully acknowledge funding from the Natural Sciences and Engineering Research Council (NSERC) of Canada through a Postgraduate Doctoral scholarship to ALL and a Discovery Grant to SAF. We thank the Nature Conservancy of Canada, Liv Monck-Whipp and Brett Norman for providing a research permit (#AG-ON-2018-153246) to do field work, and for sharing property information and general insight on Central Big Creek marsh. We thank Dean Hiler, Emily Dazé and Rosemary Martin for field assistance. Thanks to Flett Research Ltd. for providing help in interpreting the ^{210}Pb dates, and the age-depth model for core CBC3-01. Lastly, we thank Mike Lewis and Jennifer Galloway for providing insightful comments on earlier drafts of this manuscript.

References

Archer, D. (2010). *The global carbon cycle*. Princeton, NJ: Princeton University Press.

Arias-Ortiz, A., Masqué, P., Garcia-Orellana, J., Serrano, O., Mazarrasa, I., Marbà, N., Lovelock, C. E., Lavery, P. S., & Duarte, C. M. (2018). Reviews and syntheses: ^{210}Pb-derived sediment and carbon accumulation rates in vegetated coastal ecosystems – setting the record straight. *Biogeosciences*, *15*, 6791–6818. https://doi.org/10.5194/bg-15-6791-2018

Bansal, S., Lishawa, S. C., Newman, S., Tangen, B. A., Wilcox, D., Albert, D., et al. (2019). Typha (Cattail) Invasion in North American Wetlands: Biology, Regional Problems, Impacts, Ecosystem Services, and Management. *Wetlands*, *39*, 645–684. https://doi.org/10.1007/s13157-019-01174-7

Bao, K., Zhao, H., Xing, W., Lu, X., McLaughlin, N. B., & Wang, G. (2011). Carbon accumulation in temperate wetlands of Sanjiang Plain, Northeast China. *Soil Science Society of America Journal*, *75*(6), 2386. https://doi.org/10.2136/sssaj2011.0157

Barnett, P. J. (1993). *Quaternary Geology of the Long Point-Port Burwell Area* (Open File Report 5873). Ontario Geological Survey.

Barnett, P. J., Coakley, J. P., Terasmae, J., & Winn, C. E. (1985). Chronology and significance of a Holocene sedimentary profile from Clear Creek, Lake Erie shoreline, Ontario, *Canadian Journal of Earth Sciences*, *22*, 1133–1138.

Behar, F., Beaumont, V., & De B. Penteado, H. L. (2006). Rock-Eval 6 Technology: Performances and Developments. *Oil & Gas Science and Technology - Rev. IFP*, *56*(2), 111–134. https://doi.org/10.2516/ogst:2001013

Binford, M. W. (1990). Calculation and uncertainty analysis of ^{210}Pb dates for PIRLA project lake sediment cores. *Journal of Paleolimnology*, *3*, 253–267. https://doi.org/10.1007/BF00219461

Bridgham, S. D., Megonigal, P. J., Keller, J. K., Bliss, N. B., & Trettin, C. (2006). The carbon balance of North American wetlands. *Wetlands*, *26*(4), 889–916. https://doi.org/10.1672/0277-5212(2006)26[889:TCBONA]2.0.CO;2

Bridgham, S. D., Moore, T. R., Richardson, C. J., & Roulet, N. T. (2014). Errors in greenhouse forcing and soil carbon sequestration estimates in freshwater wetlands: a comment on Mitsch et al. (2013). *Landscape Ecology*, *29*(9),1481–1485.

612 Bronk Ramsey, C. (2009). Bayesian Analysis of Radiocarbon Dates. *Radiocarbon*, *51*(1),
613 Cambridge University Press, 337–360. https://doi.org/10.1017/S0033822200033865
614 Bunting, J. M., Duthie, H. C., Campbell, D. R., Warner, B. G., & Turner, L. J. (1997). A
615 palaeoecological record of recent environmental change at Big Creek Marsh, Long Point,
616 Lake Erie. *Journal of Great Lakes Research*, *23*(3), 349–368.
617 Bunting, J. M.,& Warner, B. G. (1998). Hydroseral development in southern Ontario: Patterns
618 and controls. *Journal of Biogeography*, *25*(1), 3–18. https://doi.org/10.1046/j.1365-
619 2699.1998.251195.x
620 Byun, E., Finkelstein, S. A., Cowling, S. A., & Badiou, P. (2018). Potential carbon loss
621 associated with post-settlement wetland conversion in southern Ontario, Canada. *Carbon*
622 *Balance and Management*, *13*. https://doi.org/10.1186/s13021-018-0094-4
623 Carrie, J., Sanei, H., & Stern, G. (2012). Standardisation of Rock–Eval pyrolysis for the analysis
624 of recent sediments and soils. *Organic Geochemistry*, *46*, 38–53.
625 https://doi.org/10.1016/j.orggeochem.2012.01.011
626 Chapman, L. J., & Putnam, D. F. (1984). *The Physiography of Southern Ontario* (Special
627 Volume 2). Ontario Geological Survey.
628 Ciais, P., Sabine, C., Bala, G., Bopp, L., Brovkin, V., Canadell, J., et al. (2014). Carbon and
629 other biogeochemical cycles. In T. F. Stocker, et al. (Eds.) *Climate Change 2013: The*
630 *Physical Science Basis. Contribution of Working Group I to the Fifth Assessment Report*
631 *of the Intergovernmental Panel on Climate Change*. Cambridge, UK and New York, NY:
632 Cambridge University Press.
633 Clymo, R. S. (1984). The limits to peat bog growth. *Philosophical Transactions of the Royal*
634 *Society of London. Series B, Biological Sciences*, *303*, 605–654.
635 Coakley, J.P., & Lewis, C.F.M. (1985). Postglacial lake levels in the Erie basin, in: Quaternary
636 Evolution of the Great Lakes. In P.F. Karrow, P.E. Calkin (Eds.), *Quaternary evolution*
637 *of the Great Lakes* (Special Paper, Vol. 30). St. John's, NL: Geological Association of
638 Canada.
639 Delaune, R. D., White, J. R., Elsey-Quirk, T., Roberts, H. H., & Wang, D. Q. (2018). Differences
640 in long-term vs short-term carbon and nitrogen sequestration in a coastal river delta
641 wetland: Implications for global budgets. *Organic Geochemistry*, *123*, 67–73.
642 https://doi.org/10.1016/j.orggeochem.2018.06.007

643 Dinerstein, E., Joshi, A. R., Vynne, C., Lee, A. T. L., Pharand-Deschênes, F., França, M., et al.
644 (2020). A “Global Safety Net” to reverse biodiversity loss and stabilize Earth’s climate.
645 *Science Advances*, *6*(36), eabb2824. https://doi.org/10.1126/sciadv.abb2824
646 Drever, C. R., Cook-Patton, S. C., Akhter, F., Badiou, P. H., Chmura, G. L., Davidson, S. J., et
647 al. (2021). Natural climate solutions for Canada. *Science Advances*, *7*(23), eabd6034.
648 https://doi.org/10.1126/sciadv.abd6034
649 Drexler, J. Z. (2011). Peat formation processes through the millennia in tidal marshes of the
650 Sacramento–San Joaquin Delta, California, USA. *Estuaries and Coasts*, *34*(5), 900–911.
651 https://doi.org/10.1007/s12237-011-9393-7
652 Drexler, J. Z., de Fontaine, C. S., & Brown, T. A. (2009). Peat accretion histories during the past
653 6,000 years in marshes of the Sacramento–San Joaquin Delta, CA, USA. *Estuaries and*
654 *Coasts*, *32*(5), 871–892. https://doi.org/10.1007/s12237-009-9202-8
655 Ducks Unlimited Canada (2010). Southern Ontario Wetland Conversion Analysis. Barrie, ON.
656 Environment and Climate Change Canada (2021). *1981–2010 Climate Normals & Averages*.
657 Government of Canada. Retrieved from:
658 https://climate.weather.gc.ca/climate_normals/index_e.html
659 Finkelstein, S. A., & Davis, A. M. (2006). Paleoenvironmental records of water level and
660 climatic changes from the middle to late holocene at a Lake Erie coastal wetland,
661 Ontario, Canada. *Quaternary Research*, *65*(1), 33–43.
662 https://doi.org/10.1016/j.yqres.2005.08.021
663 Finkelstein, S. A., Peros, M. C., & Davis, A. M. (2005). Late Holocene paleoenvironmental
664 change in a Great Lakes coastal wetland: integrating pollen and diatom datasets. *Journal*
665 *of Paleolimnology*, *33*(1), 1–12. https://doi.org/10.1007/s10933-004-0423-3
666 Gailis, M., Kohfeld, K. E., Pellatt, M. G., & Carlson, D. (2021). Quantifying blue carbon for the
667 largest salt marsh in southern British Columbia: Implications for regional coastal
668 management. *Coastal Engineering*, 1–35.
669 https://doi.org/10.1080/21664250.2021.1894815
670 Galloway, J. M., Swindles, G. T., Jamieson, H. E., Palmer, M., Parsons, M. B., Sanei, H., et al.
671 (2018). Organic matter control on the distribution of arsenic in lake sediments impacted
672 by ~65 years of gold ore processing in subarctic Canada. *Science of the Total*
673 *Environment*, *622–623*, 1668–1679. https://doi.org/10.1016/j.scitotenv.2017.10.048

674 Gillespie, A. W., Sanei, H., Diochon, A., Ellert, B. H., Regier, T. Z., Chevrier, D., et al. (2014).
675 Perennially and annually frozen soil carbon differ in their susceptibility to
676 decomposition: Analysis of Subarctic earth hummocks by bioassay, XANES and
677 pyrolysis. *Soil Biology and Biogeochemistry*, *68*, 106–116.
678 https://doi.org/10.1016/j.soilbio.2013.09.021
679 Goring, S., Williams, J. W., Blois, J. L., Jackson, S. T., Paciorek, C. J., Booth, R. K., et al.
680 (2012). Deposition times in the northeastern United States during the Holocene:
681 Establishing valid priors for Bayesian age models. *Quaternary Science Reviews*, *48*, 54–
682 60. https://doi.org/10.1016/j.quascirev.2012.05.019
683 Gregorich, E. G., Gillespie, A. W., Beare, M. H., Curtin, D., Sanei, H., & Yanni, S. F. (2015).
684 Evaluating biodegradability of soil organic matter by its thermal stability and chemical
685 composition. *Soil Biology and Biochemistry*, *91*, 182–191.
686 https://doi.org/10.1016/j.soilbio.2015.08.032
687 Hare, A. A., Kuzyk, Z. Z. A., Macdonald, R. W., Sanei, H., Barber, D., Stern, G. A., & Wang, F.
688 (2014). Characterization of sedimentary organic matter in recent marine sediments from
689 Hudson Bay, Canada, by Rock-Eval pyrolysis. *Organic Geochemistry*, *68*, 52–60.
690 https://doi.org/10.1016/j.orggeochem.2014.01.007
691 Heimann, M., & Reichstein, M. (2008). Terrestrial ecosystem carbon dynamics and climate
692 feedbacks. *Nature*, *451*(7176), 289–292. https://doi.org/10.1038/nature06591
693 Jones, M. C., Bernhardt, C. E., & Willard, D. A. (2014). Late Holocene vegetation, climate, and
694 land-use impacts on carbon dynamics in the Florida Everglades. *Quaternary Science*
695 *Reviews*, *90*, 90–105. https://doi.org/10.1016/j.quascirev.2014.02.010
696 Kanari, E., Cécillon, L., Baudin, F., Clivot, H., Ferchaud, F., Houot, S., Levavasseur, F., Mary,
697 B., Soucémarianadin, L., Chenu, C., & Barré, P. (2022). A robust initialization method
698 for accurate soil organic carbon simulations. *Biogeosciences*, *19*(2), 375–
699 387. https://doi.org/10.5194/bg-19-375-2022
700 Kayranli, B., Scholz, M., Mustafa, A., & Hedmark, Å. (2010). Carbon storage and fluxes within
701 freshwater wetlands: A critical review. *Wetlands*, *30*(1), 111–124.
702 https://doi.org/10.1007/s13157-009-0003-4
703 Kemp, A. C., Vane, C. H., Khan, N. S., Ellison, J. C., Engelhart, S. E., Horton, B. P., et al.
704 (2019). Testing the Utility of Geochemical Proxies to Reconstruct Holocene Coastal

705 Environments and Relative Sea Level: A Case Study from Hungry Bay, Bermuda. *Open*
706 *Quaternary*, *5*(1), 1–17. https://doi.org/10.5334/oq.49
707 Kemp, D. B., Sadler, P. M., & Vanacker, V. (2020). The human impact on North American
708 erosion, sediment transfer, and storage in a geologic context. *Nature Communications*,
709 *11*(1), 6012. https://doi.org/10.1038/s41467-020-19744-3
710 Khan, N. S., Vane, C. H., Horton, B. P., Hillier, C., Riding, J. B., & Kendrick, C. P. (2015). The
711 application of δ^{13} C, TOC and C/N geochemistry to reconstruct Holocene relative sea
712 levels and paleoenvironments in the Thames Estuary, UK. *Journal of Quaternary*
713 *Science*, *30*(5), 417–433. https://doi.org/10.1002/jqs.2784
714 Kim, J. G. (2003). Response of sediment chemistry and accumulation rates to recent
715 environmental changes in the Clear Lake watershed, California, USA. *Wetlands*, *23*(1),
716 95–103. https://doi.org/10.1672/0277-5212(2003)023[0095:ROSCAA]2.0.CO;2
717 Kolka, R., Trettin, C., Tang, W., Krauss, K., Bansal, S., Drexler, J., et al. (2018). Chapter 13:
718 Terrestrial wetlands. In N. Cavallaro et al. (Eds.) *Second State of the Carbon Cycle*
719 *Report (SOCCR2): A Sustained Assessment Report*. Washington, DC: U.S. Global
720 Change Research Program.
721 Lafargue, E., Marquis, F., & Pillot, D. (1998). Rock-Eval 6 Applications in Hydrocarbon
722 Exploration, Production, and Soil Contamination Studies. *Revue de l'Institut Français Du*
723 *Pétrole*, *53*(4), 421–437. https://doi.org/10.2516/ogst:1998036
724 Lewis, C. F. M., Breckenridge, A. J., & Teller, J. T. (2021). Reconstruction of isostatically
725 adjusted paleo-strandlines along the southern margin of the Laurentide Ice Sheet in the
726 Great Lakes, Lake Agassiz, and Champlain Sea basins. *Canadian Journal of Earth*
727 *Sciences*, 1–21. https://doi.org/10.1139/cjes-2021-0005
728 Lewis, C. F. M., Cameron, G. D. M., Anderson, T. W., Heil, C. W., & Gareau, P. L. (2012).
729 Lake levels in the Erie Basin of the Laurentian Great Lakes. *Journal of Paleolimnology*,
730 *47*(3), 493–511. https://doi.org/10.1007/s10933-012-9578-5
731 Loder, A. L., & Finkelstein, S. A. (2020). Carbon accumulation in freshwater marsh soils: A
732 synthesis for temperate North America. *Wetlands*, *40*(5), 1173–1187.
733 https://doi.org/10.1007/s13157-019-01264-6

734 Loder, A L., Gillespie, A., Ardakani, O. H., & Finkelstein, S. A. (2022). Data set for "Drivers of
735 high rates of carbon burial in a riverine-influenced freshwater marsh in the Lake Erie
736 watershed of southern Ontario, Canada". https://doi.org/10.6084/m9.figshare.19326227
737 Marrs, R. H., Marsland, E.-L., Lingard, R., Appleby, P. G., Piliposyan, G. T., Rose, R. J., et al.
738 (2019). Experimental evidence for sustained carbon sequestration in fire-managed, peat
739 moorlands. *Nature Geoscience*, *12*(2), 108–112. https://doi.org/10.1038/s41561-018-
740 0266-6
741 Martin, J. B. (2017). Carbonate minerals in the global carbon cycle. *Chemical Geology*, *449*, 58–
742 72. https://doi.org/10.1016/j.chemgeo.2016.11.029.
743 McTigue, N., Davis, J., Rodriguez, A. B., McKee, B., Atencio, A., & Currin, C. (2019). Sea
744 Level Rise Explains Changing Carbon Accumulation Rates in a Salt Marsh Over the Past
745 Two Millennia. *Journal of Geophysical Research: Biogeosciences*, *124*(10), 2945–2957.
746 https://doi.org/10.1029/2019JG005207
747 Meyers, P. A., & Teranes, J. L. (2001). Chapter 9: Sediment organic matter. In W. M. Last, J. P.
748 Smol (Eds.) *Tracking environmental change using lake sediments. Volume 2: Physical*
749 *and geochemical methods*. Dordrecht, The Netherlands: Kluwer Academic Publishers.
750 Mitsch, W. J., & Gosselink, J. G. (2015). *Wetlands* (5th edition). Hoboken, NJ: John Wiley and
751 Sons.
752 Mudd, S. M., Howell, S. M., & Morris, J. T. (2009). Impact of dynamic feedbacks between
753 sedimentation, sea-level rise, and biomass production on near-surface marsh stratigraphy
754 and carbon accumulation. *Estuarine, Coastal and Shelf Science*, *82*(3), 377–389.
755 https://doi.org/10.1016/j.ecss.2009.01.028
756 National Oceanic and Atmospheric Administration (NOAA) (2022). *NOAA Great Lakes*
757 *Environmental Research Laboratory, Great Lakes Water Level Observations*. Retrieved
758 from: https://www.glerl.noaa.gov/data/wlevels/
759 Neubauer, S. C. (2014). On the challenges of modeling the net radiative forcing of wetlands:
760 Reconsidering Mitsch et al. 2013. *Landscape Ecology*, *29*(4), 571–577.
761 https://doi.org/10.1007/s10980-014-9986-1
762 Ontario Ministry of Northern Development, Mines, Natural Resources and Forestry (2012).
763 *Quaternary geology of Ontario*. Retrieved from:
764 https://data.ontario.ca/dataset/quaternary-geology-of-ontario

765 Packalen, M. S., & Finkelstein, S. A. (2014). Quantifying Holocene variability in carbon uptake
766 and release since peat initiation in the Hudson Bay Lowlands, Canada. *The Holocene*,
767 *24*(9), 1063–1074. https://doi.org/10.1177/0959683614540728
768 Papiernik, S. K., Lindstrom, M. J., Schumacher, J. A., Farenhorst, A., Stephens, K. D.,
769 Schumacher, T. E., & Lobb, D. A. (2005). Variation in soil properties and crop yield
770 across an eroded prairie landscape. *Journal of Soil and Water Conservation*, *60*(6), 338–
771 395.
772 Pengelly, J. W., Tinkler, K. J., Parkins, W. G., & McCarthy, F. M. G. (1997). 12,600 years of
773 lake level changes, changing sills, ephemeral lakes and Niagara Gorge erosion in the
774 Niagara Peninsula and eastern Lake Erie basin. *Journal of Paleolimnology*, *17*, 377–402.
775 https://doi.org/10.1023/A:1007946401036
776 Petrescu, A. M. R., Lohila, A., Tuovinen, J. P., Baldocchi, D. D., Desai, A. R., Roulet, N. T., et
777 al. (2015). The uncertain climate footprint of wetlands under human pressure.
778 *Proceedings of the National Academy of Sciences*, *112*(15), 4594–4599.
779 https://doi.org/10.1073/pnas.1416267112
780 Peteet, D., Nichols, J., Pederson, D., Kenna, T., Chang, C., Newton, B., & Vincent, S. (2020).
781 Climate and anthropogenic controls on blue carbon sequestration in Hudson River tidal
782 marsh, Piermont, New York. *Environmental Research Letters*, *15*(6), 065001.
783 https://doi.org/10.1088/1748-9326/ab7a56
784 Pyke, M.L., Close, P.G., Dobbs, R.J., Toussaint, S., Smith, B., Cox, Z., et al. (2021). 'Clean Him
785 Up…Make Him Look Like He Was Before': Australian Aboriginal Management of
786 Wetlands with Implications for Conservation, Restoration and Multiple Evidence Base
787 Negotiations. *Wetlands*, *41*, 28. https://doi.org/10.1007/s13157-021-01410-z
788 Reddy, K.R., & Delaune, R.D. (2008). *Biogeochemistry of wetlands*. Florida: Taylor & Francis
789 Group.
790 Reimer, P., Austin, W., Bard, E., Bayliss, A., Blackwell, P., Bronk Ramsey, C., et al. (2020). The
791 IntCal20 Northern Hemisphere Radiocarbon Age Calibration Curve (0–55 cal kBP).
792 *Radiocarbon*, *62*(4), 725–757. https://doi.org/10.1017/RDC.2020.41
793 Repasch, M., Scheingross, J. S., Hovius, N., Lupker, M., Wittmann, H., Haghipour, N., et al.
794 (2021). Fluvial organic carbon cycling regulated by sediment transit time and mineral

protection. *Nature Geoscience*, *14*(11), 842–848. https://doi.org/10.1038/s41561-021-00845-7

Riley, J.L. (2013). *The once and future Great Lakes country: an ecological history*. Montreal, QC: McGill-Queen's University Press.

Rippke, M. B., Distler, M. T., & Farrell, J. M. (2010). Holocene vegetation dynamics of an upper St. Lawrence River wetland: Paleoecological evidence for a recent increase in cattail (*Typha*). *Wetlands*, *30*(4), 805–816. https://doi.org/10.1007/s13157-010-0068-0

Rogers, K., Kelleway, J. J., Saintilan, N., Megonigal, J. P., Adams, J. B., Holmquist, J. R., et al. (2019). Wetland carbon storage controlled by millennial-scale variation in relative sea-level rise. *Nature*, *567*, 91–95. https://doi.org/10.1038/s41586-019-0951-7

Saderne, V., Geraldi, N. R., Macreadie, P. I., Maher, D. T., Middelburg, J. J., Serrano, O., et al. (2019). Role of carbonate burial in Blue Carbon budgets. *Nature Communications*, *10*(1), 1106. https://doi.org/10.1038/s41467-019-08842-6

Snell, E. (1987). Wetland distribution and conversion in southern Ontario. In: *Inland Waters and Lands Dictorate* (No. 48). Ottawa, ON: Environment Canada.

Soucémarianadin, L., Cécillon, L., Chenu, C., Baudin, F., Nicolas, M., Girardin, C., & Barré, P. (2018). Is Rock-Eval 6 thermal analysis a good indicator of soil organic carbon lability? – A method-comparison study in forest soils. *Soil Biology and Biochemistry*, *117*, 108–116. https://doi.org/10.1016/J.SOILBIO.2017.10.025

Spivak, A. C., Sanderman, J., Bowen, J. L., Canuel, E. A., & Hopkinson, C. S. (2019). Global-change controls on soil-carbon accumulation and loss in coastal vegetated ecosystems. *Nature Geoscience*, *12*(9), 685–692. https://doi.org/10.1038/s41561-019-0435-2

Strachan, I.B., Nugent, K.A., Crombie, S., & Bonneville, M.C. (2015). Carbon dioxide and methane exchange at a cool-temperate freshwater marsh. *Environmental Research Letters*, *10*(6), 065006. https://doi.org/10.1088/1748-9326/10/6/065006

Van de Broek, M., Temmerman, S., Merckx, R., & Govers, G. (2016). Controls on soil organic carbon stocks in tidal marshes along an estuarine salinity gradient. *Biogeosciences*, *13*(24), 6611–6624. https://doi.org/10.5194/bg-13-6611-2016

Van de Broek, M., Vandendriessche, C., Poppelmonde, D., Merckx, R., Temmerman, S., & Govers, G. (2018). Long-term organic carbon sequestration in tidal marsh sediments is

825 dominated by old-aged allochthonous inputs in a macrotidal estuary. *Global Change*
826 *Biology*, *24*(6), 2498–2512. https://doi.org/10.1111/gcb.14089
827 Young, D. M., Baird, A. J., Charman, D. J., Evans, C. D., Gallego-Sala, A. V., Gill, P. J., et al.
828 (2019). Misinterpreting carbon accumulation rates in records from near-surface peat.
829 *Scientific Reports*, *9*(1), 17939. https://doi.org/10.1038/s41598-019-53879-8
830 Yu, L., Huang, Y., Sun, F., & Sun, W. (2017). A synthesis of soil carbon and nitrogen recovery
831 after wetland restoration and creation in the United States. *Scientific Reports*, *7*(1), 7966.
832 https://doi.org/10.1038/s41598-017-08511-y
833 Yu, Z., McAndrews, J. H., & Siddiqi, D. (1996). Influences of Holocene climate and water levels
834 on vegetation dynamics of a lakeside wetland. *Canadian Journal of Botany*, *74*, 1602–
835 1615. https://doi.org/10.1139/b96-194
836 Yu, Z., Loisel, J., Brosseau, D.P., Beilman, D.W., & Hunt, S.J. (2010). Global peatland
837 dynamics since the Last Glacial Maximum. *Geophysical Research Letters*, *37*, L13402.
838 https://doi.org/10.1029/2010GL043584
839 Zamanian, K., Zhou, J., & Kuzyakov, Y. (2021). Soil carbonates: The unaccounted,
840 irrecoverable carbon source. *Geoderma*, *384*, 114817.
841 https://doi.org/10.1016/j.geoderma.2020.114817
842 Zhang, Y., Gao, Y., Zhang, Y., Huang, D., Li, X., McLaughlin, N., Zhang, X., Chen, X., Zhang,
843 S., Gregorich, E., & Liang, A. (2023). Linking Rock-Eval parameters to soil
844 heterotrophic respiration and microbial residues in a black soil. *Soil Biology and*
845 *Biochemistry*, *178*, 108939. https://doi.org/10.1016/j.soilbio.2023.108939
846 Zoltai, S.C. (1988). Chapter 1: Wetland Environments and Classification. In *Wetlands of*
847 *Canada*. Montreal, QC: Polyscience Publications Inc.

Figures and tables

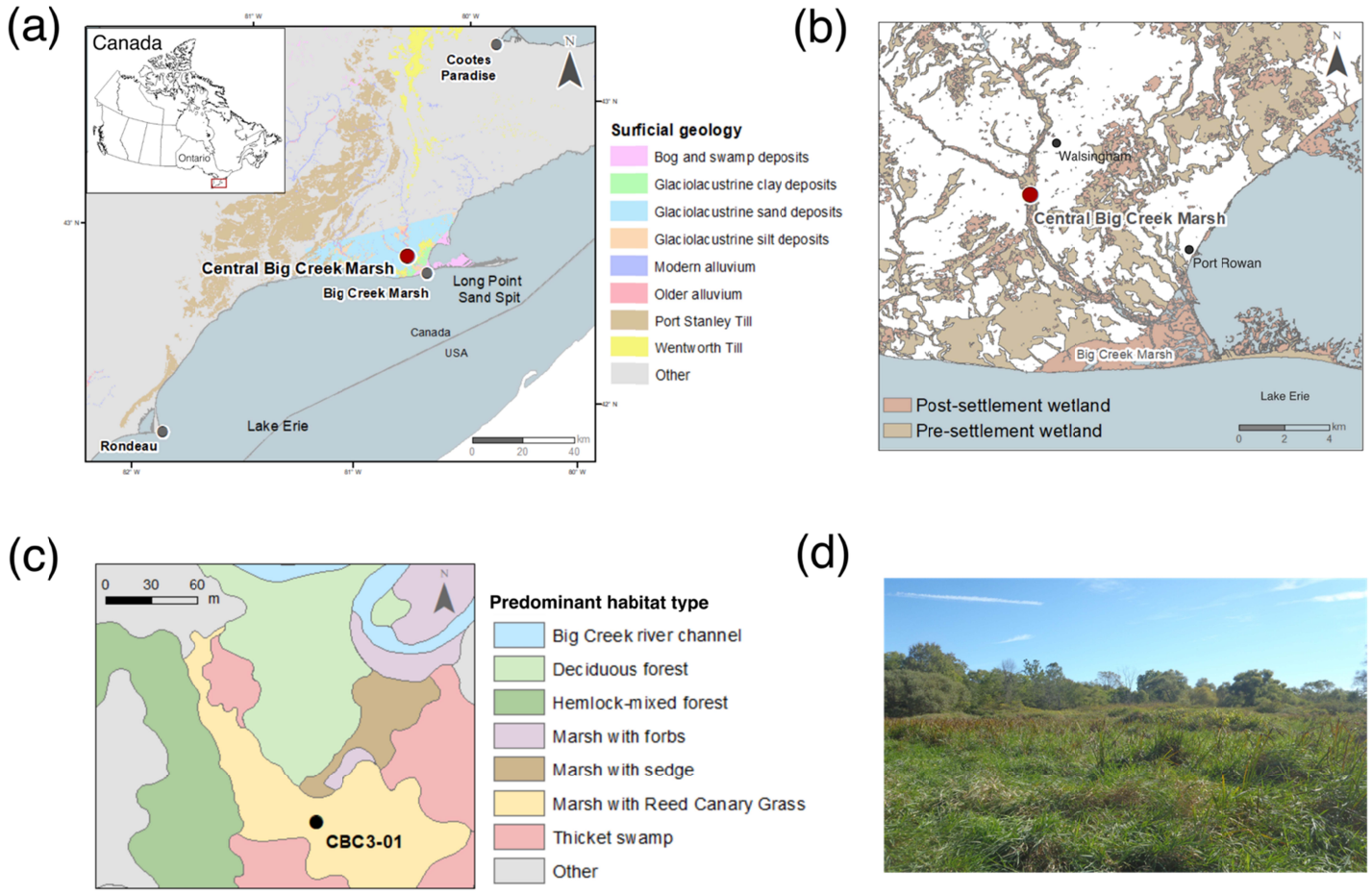

Figure 1. Maps and photos of Central Big Creek Marsh where core CBC3-01 was retrieved in southern Ontario, Canada. Central Big Creek Marsh is situated on the traditional lands of the Attawandaron, Haudenosaunee and the Anishinaabe First Nations, and within the Treaty lands ('Between the Lakes Purchase') of the Mississaugas of the Credit. a) Location of Central Big Creek Marsh relative to Ontario, Canada, and other local freshwater marshes (Rondeau, Big Creek Marsh and Cootes Paradise). Surficial geology is shown for the Big Creek watershed and other areas of Norfolk County as mapped in the Quaternary Geology of Ontario dataset (Ontario Ministry of Northern Development, Mines, Natural Resources and Forestry, 2012). b) Location of Central Big Creek Marsh within the Big Creek watershed. Both pre-European settlement wetlands (i.e., wetland that has been drained and altered since European settlement in the region) and post-European settlement wetlands (i.e., wetland that remains intact at present day) are shown from Byun et al. (2018). All present-day wetlands are considered to have also been wetlands during the pre-settlement period. c) Predominant habitat types as identified and mapped by the Nature Conservancy of Canada in 2010 within the Central Big Creek Marsh, and location where CBC3-01 was extracted. d) Ground-level image of Central Big Creek Marsh.

Table 1. AMS radiocarbon dates from sediment core CBC3-01, collected from Central Big Creek Marsh in Southern Ontario, Canada. Dates were calibrated using OxCal 4.4 with the IntCal20 calibration curve (Bronk Ramsey, 2009; Reimer et al., 2020). Raw radiocarbon dates can be used to generate age-depth model with 95% confidence intervals in rbacon (Figure 2(b)).

Depth (cm)	**Material dated**	**^{14}C age (yr BP)**	**Calibrated age 2σ (yr BP)**	**Median age (yr BP)**	**Lab number**
52–54	Wood	145 ± 26	281–170 (40 %) 154–126 (10 %) 120–56 (27 %) 47 (19 %)	140	UOC-12338
78–80	Wood	463 ± 26	537–491 (95 %)	510	UOC-15387
98–100	Wood	506 ± 25	549–506 (95 %)	530	UOC-14899
126–128	Wood	1,844 ± 26	1,826–1,704 (95 %)	1,750	UOC-12339
216–218	Wood	3,603 ± 26	3,976–3,844 (95 %)	3,910	UOC-12340
270–272	Wood	4,140 ± 25	4,823–4,745 (31 %) 4,734–4,572 (65 %) 4,538–4,535 (<1 %)	4,690	UOC-12341
286–288	Wood	4,301 ± 27	4,960–4,929 (9 %) 4,912–4,899 (2 %) 4,887–4,830 (85 %)	4,860	UOC-12342
384–386	Twig	4,692 ± 23	5,477–5,435 (25 %) 5,422–5,321 (70 %)	5,380	UOC-12343
400–402	Plant macrofossil	4,634 ± 26	5,462–5,375(74 %) 5,358–5,346 (3 %) 5,333–5,308 (19 %)	5,410	UOC-13435
426–429	Wood pieces	4,991 ± 27	5,884–5,825 (14 %) 5,754–5,650 (73 %) 5,631–5,604 (8 %)	5,710	UOC-13436

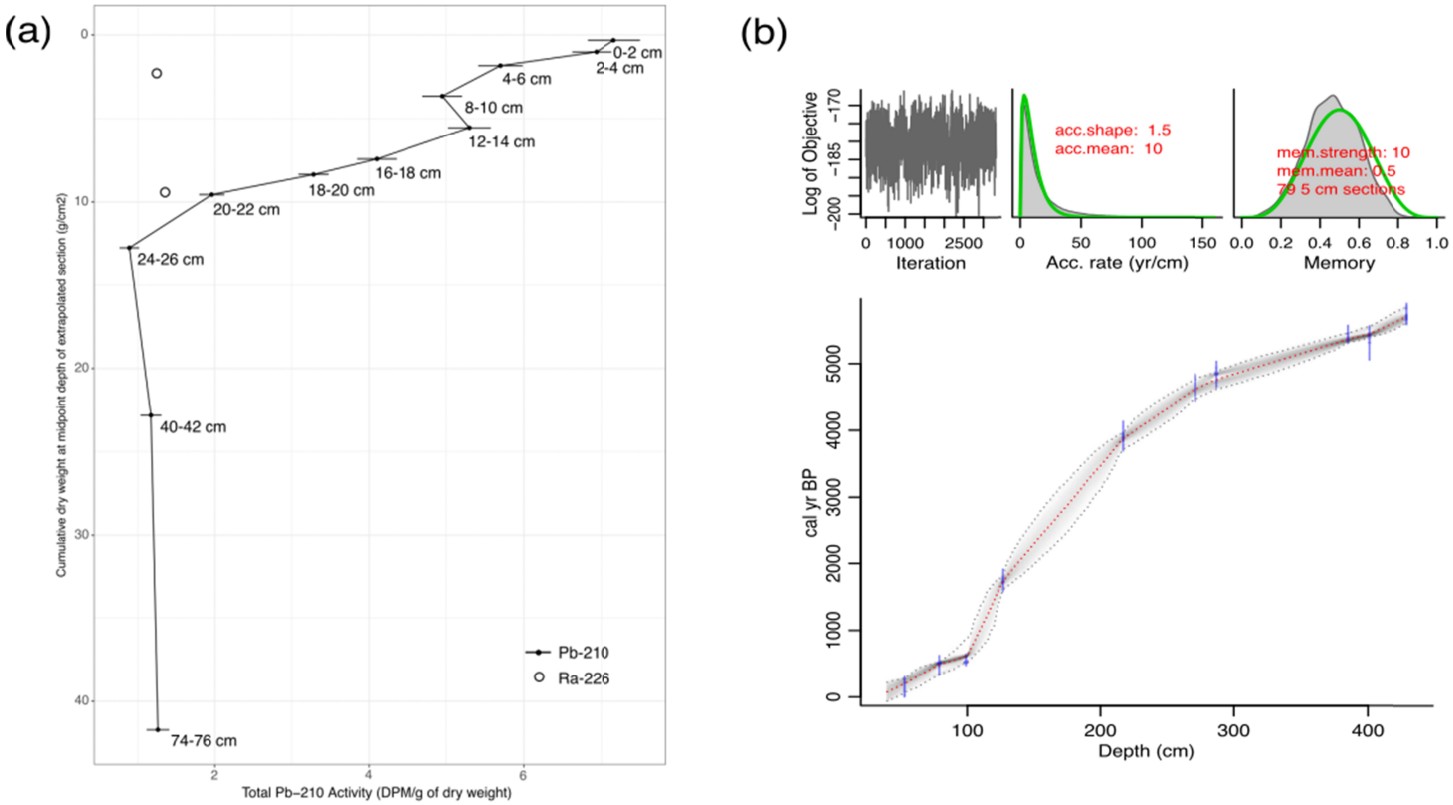

Figure 2. (a) Total ^{210}Pb and ^{226}Ra activities (DPM g^{-1} of dry weight) plotted against the cumulative dry weight at the midpoint depth for several extrapolated sections (g cm^{-2}) from CBC3-01. Error bars represent +/- one standard deviation. Errors for ^{226}Ra activities are <0.08 DPM g^{-1} and not visible at the scale of the plot. Sediments deposited between 0–20 cm depth are dated using ^{210}Pb age modelling. (b) Bayesian age-depth model developed for 40–429 cm of CBC3-01 using ^{14}C dates in rbacon. Confidence intervals (95%) are shown in the grey shading. Sediments deposited between 20–40 cm are undated.

876

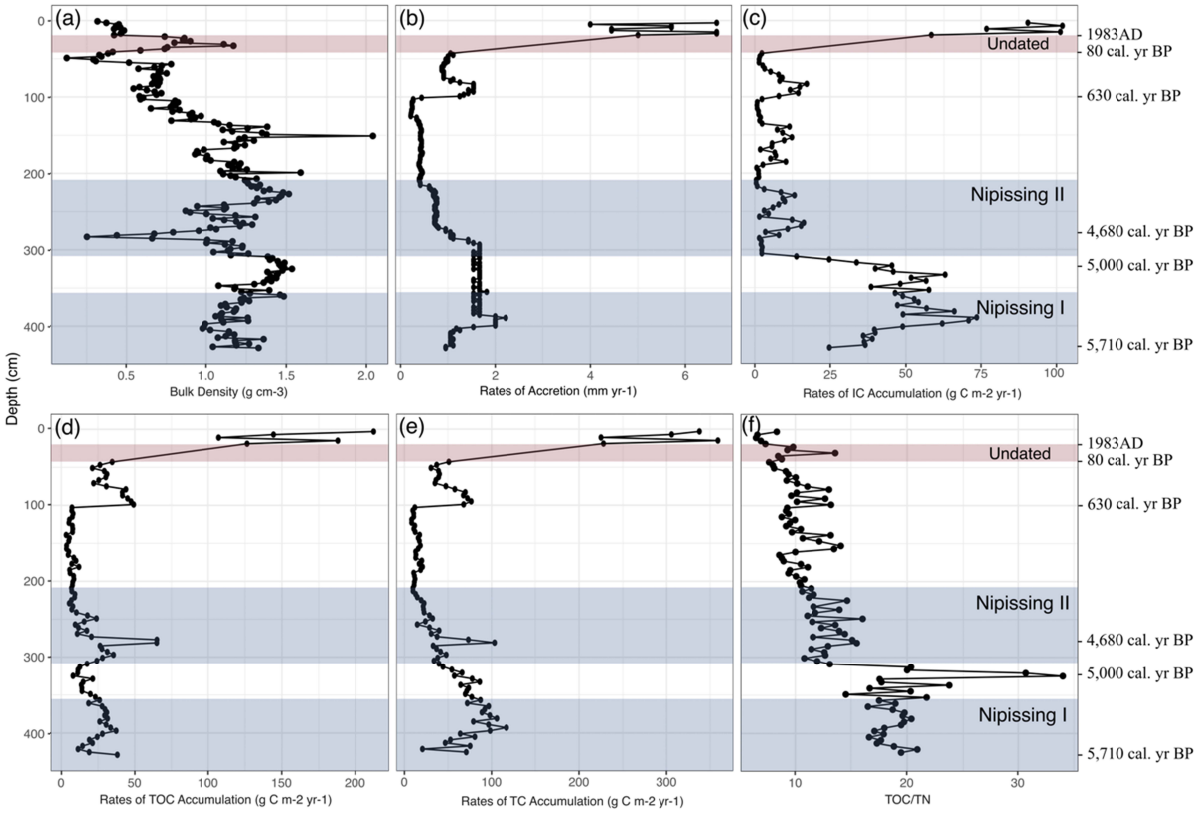

877

878 **Figure 3.** Bulk density (a), rates of accretion (b), rates of inorganic carbon (IC) accumulation (via programmed
879 pyrolysis; c), rates of total organic carbon (TOC) accumulation (via programmed pyrolysis; (d)), rates of total
880 carbon (TC) accumulation (via CHN elemental analyses with precision range of 0.5% for TC content; (e)) and
881 TOC/TN ratios (via programmed pyrolysis for TOC and CHN elemental analyses for TN; (f)). Red boxes
882 highlight undated sediments that are disturbed, and blue boxes highlight sediments deposited during Nipissing I
883 and II. Mean calibrated ages derived from the age-depth model (Figure 2(b)) for key transitions are shown on
884 the right-hand margin in the geochemical proxies plotted here. Radiocarbon dates are provided in Table 1.

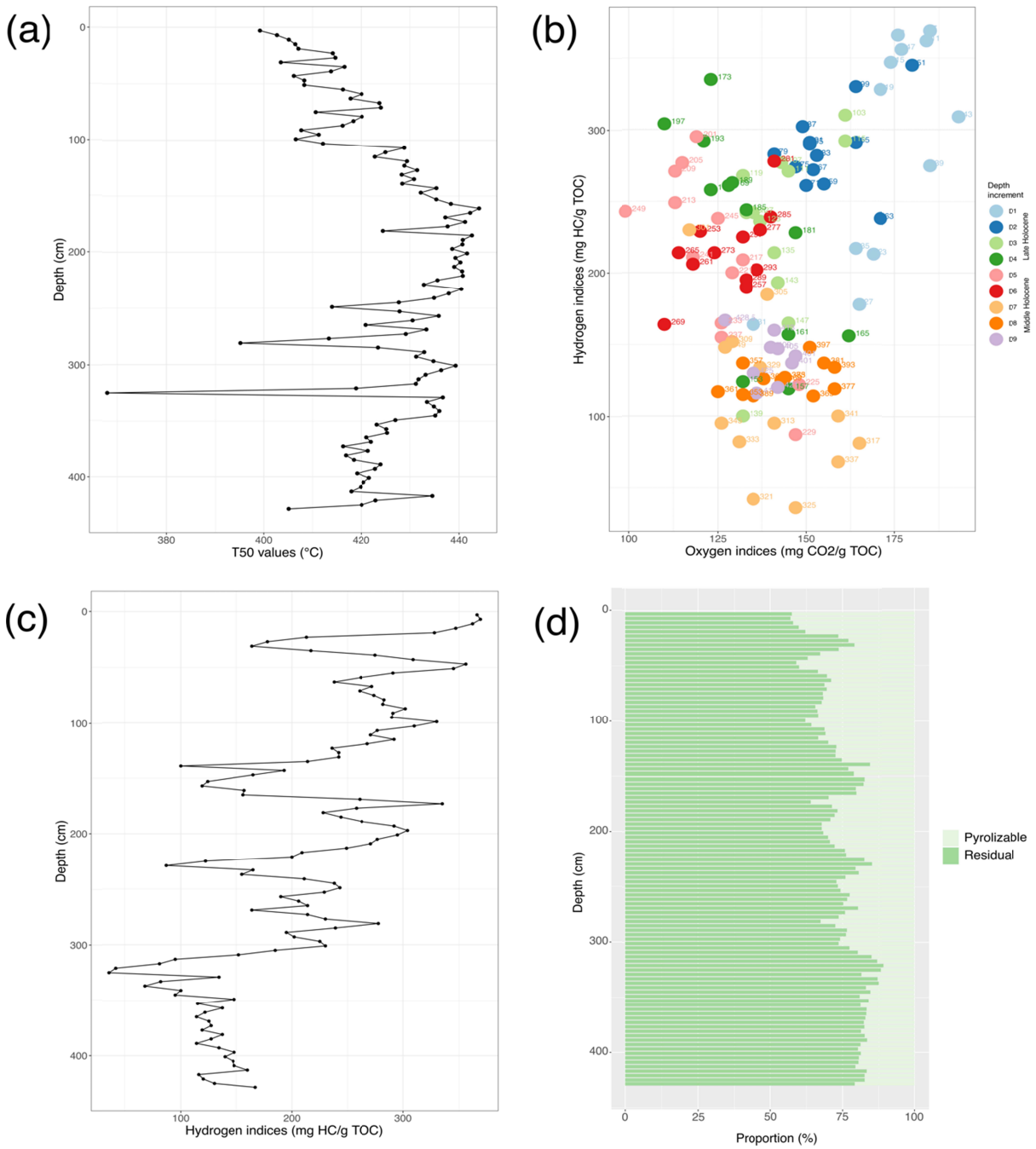

Figure 4. Results from programmed pyrolysis on core CBC3-01. (a) Temperatures (°C) at which half of carbon fraction was released from soil samples (T50 values) plotted against depth. (b) Pseudo van Krevelen plot of hydrogen versus oxygen index values. Numbers adjacent to points on the plot denote the mid-depth (in cm) of soil samples from the 430-cm core. D1 = 0–50 cm, D2 = 50–100 cm, D3 = 100–150 cm, D4 = 150–200 cm, D5 = 200–250 cm, D6 = 250–300cm, D7 = 300–350 cm, D8 = 350–400 cm, D9 = 400–429 cm. (c) Hydrogen indices plotted against depth. (d) Proportions (%) of pyrolizable (i.e., generative organic carbon) and residual (non-generative organic carbon) fractions of organic carbon in relation to total organic carbon contents plotted against depth.

Figure 1.

(a)

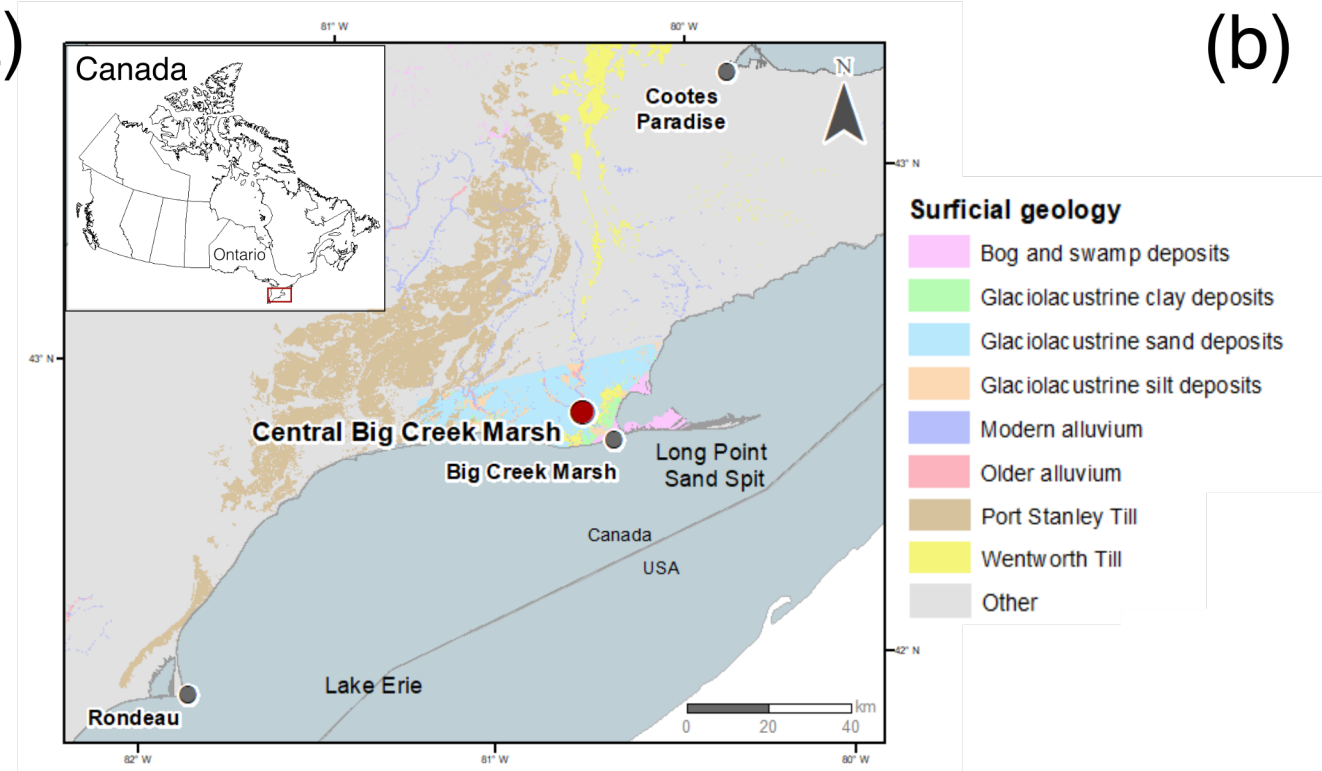
Canada
Ontario
81° W
80° W
43° N
42° N
N
Cootes Paradise
Central Big Creek Marsh
Big Creek Marsh
Long Point Sand Spit
Canada
USA
Lake Erie
Rondeau
82° W
0 20 40 km
Surficial geology
Bog and swamp deposits
Glaciolacustrine clay deposits
Glaciolacustrine sand deposits
Glaciolacustrine silt deposits
Modern alluvium
Older alluvium
Port Stanley Till
Wentworth Till
Other

(b)

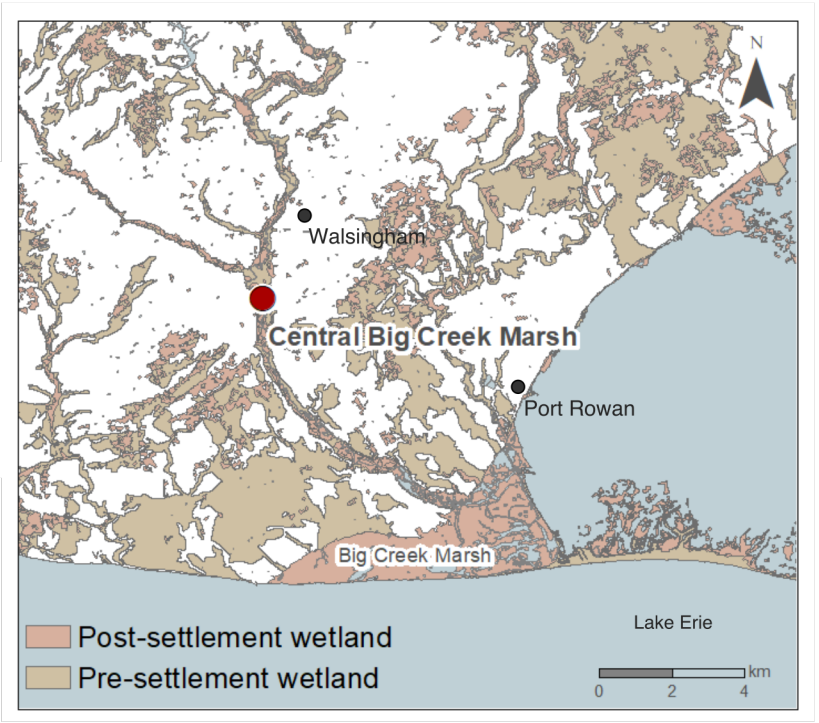
N
Walsingham
Central Big Creek Marsh
Port Rowan
Big Creek Marsh
Lake Erie
Post-settlement wetland
Pre-settlement wetland
0 2 4 km

(c)

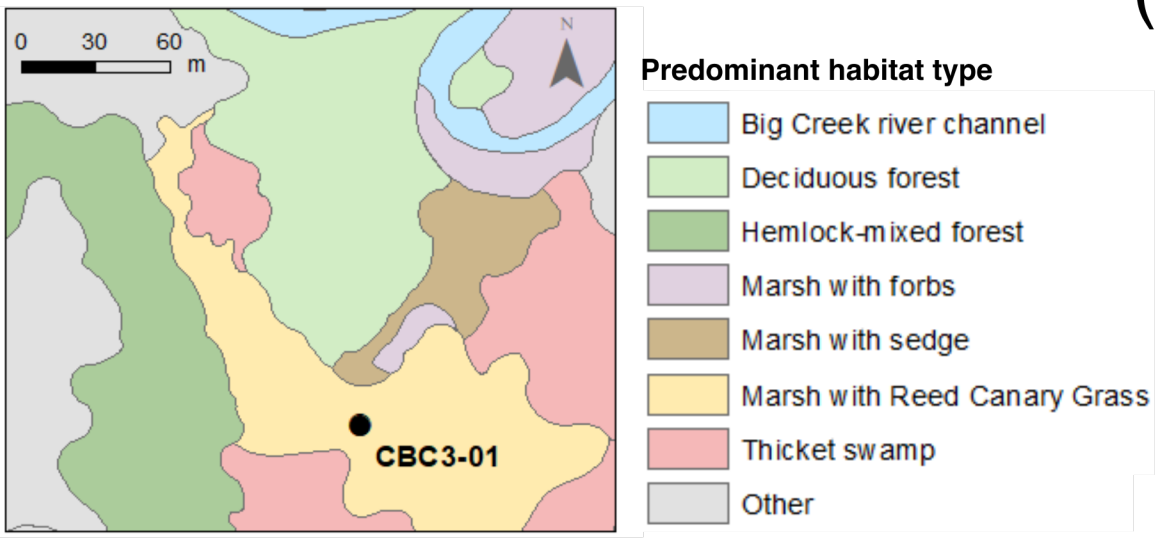
0 30 60 m
N
CBC3-01
Predominant habitat type
Big Creek river channel
Deciduous forest
Hemlock-mixed forest
Marsh with forbs
Marsh with sedge
Marsh with Reed Canary Grass
Thicket swamp
Other

(d)

Figure 2.

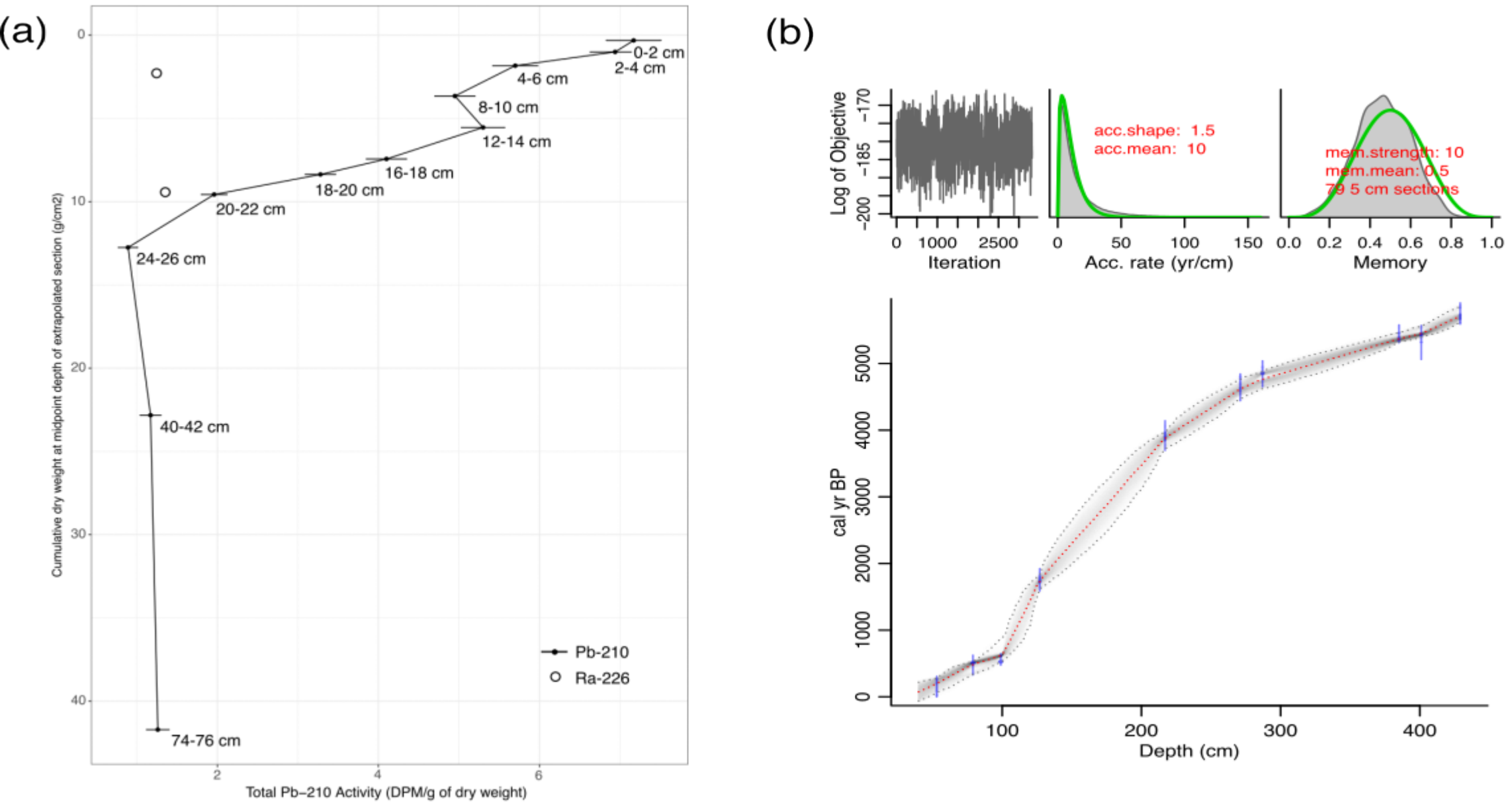
(a)
0-2 cm
2-4 cm
4-6 cm
8-10 cm
12-14 cm
16-18 cm
18-20 cm
20-22 cm
24-26 cm
40-42 cm
74-76 cm
Pb-210
Ra-226
Cumulative dry weight at midpoint depth of extrapolated section (g/cm2)
Total Pb−210 Activity (DPM/g of dry weight)
(b)
Log of Objective
Iteration
acc.shape: 1.5
acc.mean: 10
Acc. rate (yr/cm)
mem.strength: 10
mem.mean: 0.5
79 5 cm sections
Memory
cal yr BP
Depth (cm)

Figure 3.

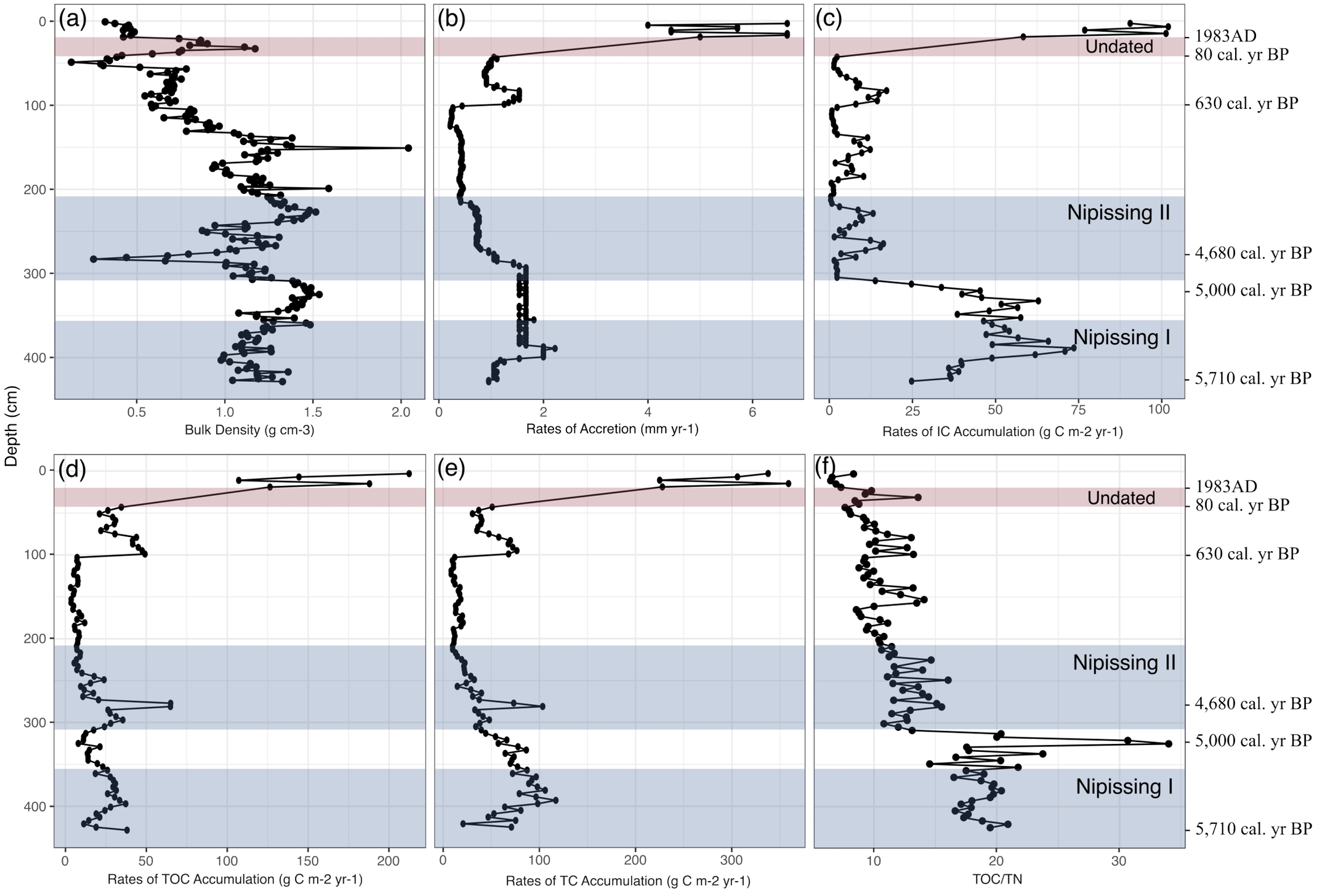
(a)
(b)
(c)
(d)
(e)
(f)
Undated
Nipissing II
Nipissing I
1983AD
80 cal. yr BP
630 cal. yr BP
4,680 cal. yr BP
5,000 cal. yr BP
5,710 cal. yr BP
Bulk Density (g cm-3)
Rates of Accretion (mm yr-1)
Rates of IC Accumulation (g C m-2 yr-1)
Rates of TOC Accumulation (g C m-2 yr-1)
Rates of TC Accumulation (g C m-2 yr-1)
TOC/TN

Figure 4.

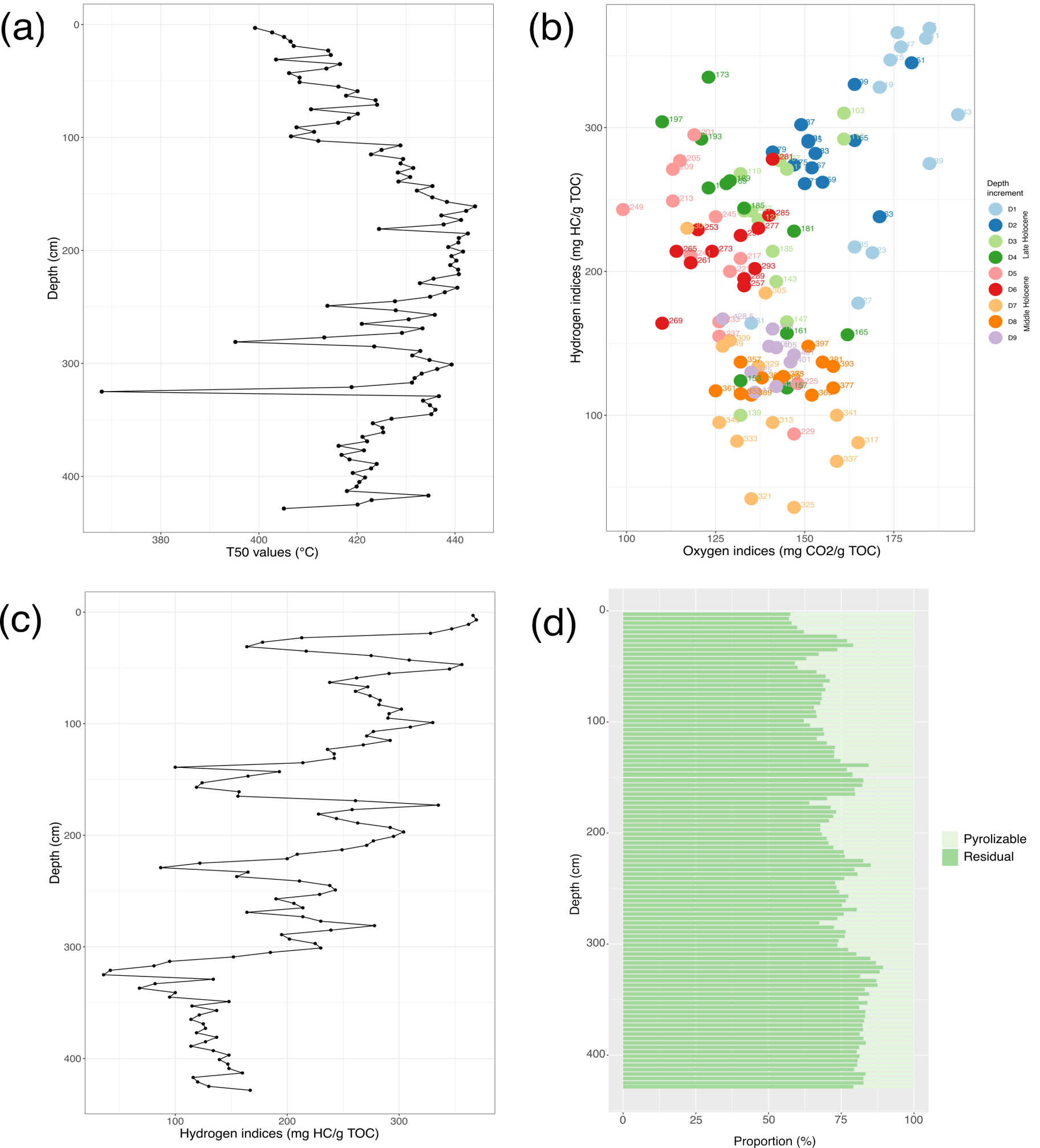
(a)
Depth (cm)
T50 values (°C)
(b)
Hydrogen indices (mg HC/g TOC)
Oxygen indices (mg CO2/g TOC)
Depth increment
D1
D2
D3
D4
D5
D6
D7
D8
D9
Late Holocene
Middle Holocene
(c)
Depth (cm)
Hydrogen indices (mg HC/g TOC)
(d)
Depth (cm)
Proportion (%)
Pyrolizable
Residual